HHS Public Access

Author manuscript

Cell Rep. Author manuscript; available in PMC 2022 February 24.

Published in final edited form as:

Cell Rep. 2022 February 08; 38(6): 110321. doi:10.1016/j.celrep.2022.110321.

Neuronal GPCR NMUR-1 regulates distinct immune responses to different pathogens

Phillip Wibisono[1], **Shawndra Wibisono**[1], **Jan Watteyne**[2], **Chia-Hui Chen**[1], **Durai Sellegounder**[1], **Isabel Beets**[2], **Yiyong Liu**[1,3,*], **Jingru Sun**[1,4,*]

[1]Department of Translational Medicine and Physiology, Elson S. Floyd College of Medicine, Washington State University, Spokane, WA, USA

[2]Department of Biology, KU Leuven, Leuven, Belgium

[3]Genomics Core, Washington State University, Spokane, WA, USA

[4]Lead contact

SUMMARY

A key question in current immunology is how the innate immune system generates high levels of specificity. Using the *Caenorhabditis elegans* model system, we demonstrate that functional loss of NMUR-1, a neuronal G-protein-coupled receptor homologous to mammalian receptors for the neuropeptide neuromedin U, has diverse effects on *C. elegans* innate immunity against various bacterial pathogens. Transcriptomic analyses and functional assays reveal that NMUR-1 modulates *C. elegans* transcription activity by regulating the expression of transcription factors involved in binding to RNA polymerase II regulatory regions, which, in turn, controls the expression of distinct immune genes in response to different pathogens. These results uncover a molecular basis for the specificity of *C. elegans* innate immunity. Given the evolutionary conservation of NMUR-1 signaling in immune regulation across multicellular organisms, our study could provide mechanistic insights into understanding the specificity of innate immunity in other animals, including mammals.

Graphical Abstract

*Correspondence: yiyong.liu@wsu.edu (Y.L.), jingru.sun@wsu.edu (J.S.).

AUTHOR CONTRIBUTIONS

P.W., S.W., J.W., C.-H.C., D.S., Y.L., and I.B. designed and performed experiments and analyzed data. J.S. designed experiments and analyzed data. Y.L., J.S., and P.W. wrote the paper.

SUPPLEMENTAL INFORMATION

Supplemental information can be found online at https://doi.org/10.1016/j.celrep.2022.110321.

DECLARATION OF INTERESTS

The authors declare no competing interests.

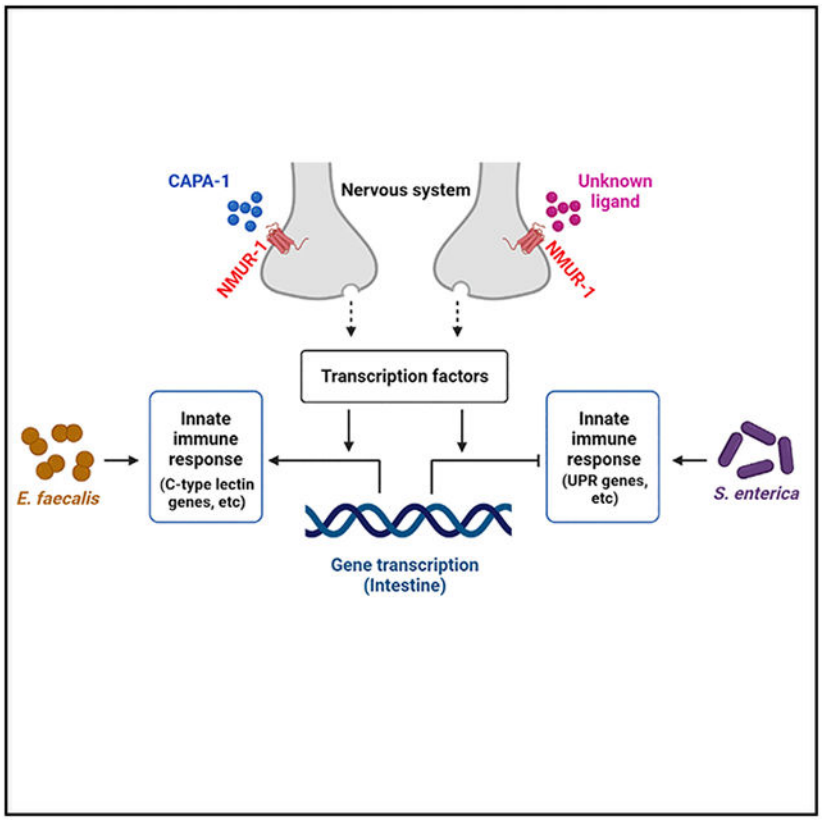

In brief

Wibisono et al. discover that neuronal GPCR NMUR-1 modulates *C. elegans* transcription activity by regulating the expression of transcription factors, which, in turn, controls the expression of distinct immune genes in response to different pathogens. These results uncover a molecular basis for the specificity of *C. elegans* innate immunity.

INTRODUCTION

The pathogen-triggered host immune response is a multilayered process programmed to fight invading microorganisms and maintain healthy homeostasis. There are two types of immune systems: the innate immune system and the adaptive immune system. Traditionally, immune specificity was ascribed to the adaptive immune system, whereas the innate immune response was thought to be non-specific. However, increasing evidence indicates that the innate immune system can also generate high levels of specificity (Milling, 2019). In vertebrates, a diverse array of pattern recognition receptors (PRRs), such as the Toll-like receptors (TLRs), NOD-like receptors, retinoic acid-inducible gene-I-like receptors, and C-type lectins, recognize various pathogen-associated molecular patterns (PAMPs) and mediate a broad pattern of specificity (Pees et al., 2016). The diversity of ligand binding can be further expanded by the formation of receptor homodimers or heterodimers through interactions with other PRR co-receptors (Tan et al., 2014). In addition to controlling immune activation through specific receptor-ligand binding, innate immunity

is also tightly regulated by the nervous system to ensure that appropriate responses are mounted against specific pathogens. Such regulation is critical because insufficient immune responses can exacerbate infection and excessive immune responses can lead to prolonged inflammation, tissue damage, or even death (Steinman, 2004; Sternberg, 2006). The mechanisms underlying neuroimmune regulation, however, are not well understood and are difficult to decipher due to the high degree of complexity of the nervous and immune systems in most model organisms. Overall, the molecular basis responsible for the specificity of innate immunity in vertebrates remains unclear and is largely understudied, likely because such specificity is overshadowed by the concomitant adaptive immune response.

Unlike vertebrates, most invertebrates do not have an adaptive immune system and rely solely on innate immunity to defend themselves against pathogen infection, yet they can still differentiate between different pathogens (Pees et al., 2016). For example, *Drosophila melanogaster* possesses a repertoire of receptors that mediate the distinction of different types of pathogens and fungi (Cherry and Silverman, 2006). Alternative splicing of exons of the Dscam protein in insects generates thousands of isoforms that are potentially involved in pathogen recognition and resistance (Schulenburg et al., 2007). Moreover, in both *D. melanogaster* and *Caenorhabditis elegans*, brief pre-exposure of animals to a pathogen (termed priming or conditioning) provides strong protection against a subsequent challenge with an otherwise lethal dose of the same pathogen (Sharrock and Sun, 2020). These studies demonstrate that invertebrate innate immune systems can generate high levels of specificity, although the underlying mechanisms remain poorly understood. Nonetheless, the invertebrate systems allow for studies of the specificity of innate immunity without the confounding variability from adaptive immunity. In invertebrate organisms, the limited genetic diversity of PRRs and immune effectors is likely insufficient to explain the high levels of specificity (Schulenburg et al., 2007). This is exemplified by the case of *C. elegans*. The nematode genome does not encode the majority of known PRRs, and its sole TLR protein, TOL-1, does not seem to play key roles in immunity (Sun et al., 2016). However, *C. elegans* can still discern different pathogens and launch distinct immune responses against them (Irazoqui et al., 2010; Zarate-Potes et al., 2020). Different infections induce both pathogen-specific and shared immune genes in the worm (Wong et al., 2007; Zarate-Potes et al., 2020). While how the *C. elegans* immune system identifies specific pathogens remains elusive, several key studies have revealed that neural regulation of immunity has homologous occurrence in the nematode (Anyanful et al., 2009; Kawli and Tan, 2008; Pradel et al., 2007; Reddy et al., 2009; Styer et al., 2008; Sun et al., 2011; Zhang et al., 2005), which could control appropriate immune responses to different pathogens. The characteristics of *C. elegans*, such as the simplicity of its nervous and immune systems, genetic tractability, invariant lineage, effectiveness of RNA interference (RNAi), and a transparent body that allows for the monitoring of gene expression, make this organism uniquely suited for studying neural regulation of immunity. Indeed, such research in *C. elegans* is at the forefront of the field and has revealed unprecedented details regarding the molecules, cells, and signaling pathways involved in neural regulation of immunity (reviewed in Liu and Sun, 2021). For example, we have described an octopaminergic neuroimmune regulatory circuit in great detail (Liu et al., 2016; Sellegounder et al., 2018;

Sun et al., 2011, 2012) as well as a neural-cuticle defense regulatory circuit mediated by the neuropeptide receptor NPR-8 (Sellegounder et al., 2019). Others have also revealed serotonergic, dopaminergic, cholinergic, and neuropeptidergic immunoregulatory pathways that control innate immune responses to various pathogens (reviewed in Liu and Sun, 2021). These studies have greatly improved our understanding of complex neuroimmune controlling mechanisms.

While the aforementioned *C. elegans* studies showed how the nervous system regulates immunity against certain pathogens, they did not address whether or how such regulation generates specificity against different pathogens. During our work on neuroimmune regulation in *C. elegans*, we observed that functional loss of NMUR-1, a neuronal G-protein-coupled receptor (GPCR) homologous to mammalian receptors for the neuropeptide neuromedin U (NMU), had diverse effects on the survival of *C. elegans* exposed to various bacterial pathogens. Furthermore, an earlier study by Alcedo and colleagues showed that an *nmur-1* null mutation affected the lifespan of *C. elegans* fed different *Escherichia coli* food sources, and that the effect was dependent upon the type of *E. coli* lipopolysaccharide (LPS) structures (Maier et al., 2010). These findings indicate that NMU/NMUR-1 signaling might mediate the specificity of immune responses to different pathogens. NMU is known to have roles in regulating immune responses in addition to its functions regulating smooth muscle contractions in the uterus, reducing food intake and weight, and modifying ion transport (Martinez and O'Driscoll, 2015; Ye et al., 2021). Indeed, three independent studies in mice demonstrated that NMU from enteric neurons directly activates type 2 innate lymphoid cells through NMUR1 to drive anti-parasitic immunity (Cardoso et al., 2017; Klose et al., 2017; Wallrapp et al., 2017). In the current study, we have discovered that NMUR-1 modulates *C. elegans* transcriptional activity by regulating the expression of transcription factors, which, in turn, controls the expression of distinct immune genes in response to different pathogens. Our study has uncovered a molecular basis for the specificity of *C. elegans* innate immunity that could potentially provide mechanistic insights into understanding the specificity of innate immune responses in vertebrates.

RESULTS

Functional loss of NMUR-1 differentially affects *C. elegans* survival against various bacterial pathogens

Functional loss of NMUR-1 has distinct effects on the lifespan of *C. elegans* fed different *E. coli* food sources, and such effects are dependent upon the type of *E. coli* LPS structures (Maier et al., 2010). Given the toxic and immunogenic nature of LPS (Mazgaeen and Gurung, 2020), these LPS-dependent lifespan phenotypes suggest that NMUR-1 might mediate distinct immune responses to different pathogens. To test this notion, we examined the susceptibility of wild-type *N2* and *nmur-1* null animals (*nmur-1*(*ok1387*) strain) to six paradigmatic pathogens that included three Gram-negative bacteria (*Salmonella enterica* strain SL1344, *Pseudomonas aeruginosa* strain PA14, and *Yersinia pestis* strain KIM5) and three Gram-positive bacteria (*Enterococcus faecalis* strain OG1RF, *Microbacterium nematophilum* strain CBX102, and *Staphylococcus aureus* strain MSSA476). Compared with wild-type animals, *nmur-1*(*ok1387*) animals exhibited enhanced survival against *S.*

enterica and *Y. pestis*, reduced survival against *E. faecalis*, and showed no differences in survival against *P. aeruginosa*, *M. nematophilum*, and *S. aureus* (Figures 1 and S1). In addition, with two commonly used worm food sources, namely, *E. coli* strains OP50 and HT115, we found that the *nmur-1* mutation improved worm survival against OP50 but had no effect against HT115 (Figures 1 and S1), an observation in agreement with a previous study by Alcedo and colleagues (Maier et al., 2010). These distinct effects of the *nmur-1* mutation on survival, which appeared to be unrelated to the Gram-negative or Gram-positive groups, indicate that NMUR-1 plays diverse roles in *C. elegans* defense against various pathogens. To test whether such effects of the *nmur-1* mutation are strain specific, we performed survival assays against the six pathogens using another *nmur-1* null strain (*nmur-1*(*its1672*)) that was generated using a common CRISPR/Cas9 genome-editing protocol (Watteyne et al., 2020). The results were consistent with those of *nmur-1*(*ok1387*) animals (Figure S2), indicating that the effects on survival are not strain specific but are caused by the general lack of NMUR-1 function.

There are many factors affecting the pathogenesis of the aforementioned bacteria besides being Gram-negative or Gram-positive. For example, each pathogen can produce a unique set of virulence factors that promote pathogenicity through different mechanisms (Peterson, 1996). The diverse effects of NMUR-1 on *C. elegans* survival suggest that it could have multiple physiological functions in the nematode's defense against these bacteria. Given NMUR-1's potential versatility in function, we sought to gain insights into NMUR-1's functionality by focusing on its roles in defense against *E. faecalis* and *S. enterica*, two pathogens that have opposite effects on the survival of *nmur-1* mutant animals (reduced survival against *E. faecalis* but improved survival against *S. enterica*) (Figure 1). We now describe our study using these two pathogens as infecting agents.

Pathogen avoidance behavior does not contribute to the altered survival of *nmur-1*(*ok1387*) animals exposed to *E. faecalis* or *S. enterica*

As described above, compared with wild-type animals, *nmur-1*(*ok1387*) animals exhibited altered survival following exposure to *E. faecalis* or *S. enterica* (Figure 1). However, no differences in survival were observed between mutant and wild-type animals when they were fed worm food *E. coli* strain HT115 (Figure 1), heat-killed *E. faecalis*, or heat-killed *S. enterica* (Figure S3). These results indicate that the *nmur-1* mutation affects *C. elegans* defense against living pathogens without impacting the nematode's basic lifespan. The altered survival of mutant animals could be due to pathogen avoidance behavior, a known mechanism of *C. elegans* defense (Meisel and Kim, 2014). To test this possibility, we measured animal survival using full-lawn assays in which the agar plates were completely covered by pathogenic bacteria to eliminate pathogen avoidance. Consistent with our original (partial-lawn) survival assays, we observed that *nmur-1*(*ok1387*) animals exposed to *E. faecalis* died at a faster rate than wild-type controls, whereas mutants exposed to *S. enterica* died at a slower rate than wild-type controls (Figure S4). These results suggest that lawn avoidance is not the reason for the altered survival observed in *nmur-1* mutants. We next conducted lawn occupancy behavioral assays to compare the magnitude of pathogen avoidance between wild-type and *nmur-1*(*ok1387*) animals. In these assays, a small lawn of pathogenic bacteria was seeded in the center of an agar plate, and a set number of

synchronized young adult animals were placed on the lawn. The numbers of animals that stayed on and off the lawn were then counted at five time points over a period of 36 h. Compared with wild-type animals, *nmur-1*(*ok1387*) animals overall did not show significant differences in the magnitudes of pathogen avoidance (Figures 1D and 1E). Taken together, these data suggest that pathogen avoidance behavior does not play a role in the altered survival of *nmur-1*(*ok1387*) animals exposed to *E. faecalis* or *S. enterica*.

Functional loss of NMUR-1 changes intestinal accumulation of *E. faecalis* and *S. enterica*

Certain mutations in *C. elegans* can change pathogen accumulation in the intestine, leading to altered resistance to infection (Fuhrman et al., 2009). To examine whether the *nmur-1* mutation affects bacterial accumulation, we used GFP-tagged *E. faecalis* to visualize accumulated bacteria in the nematode's intestine. Our results showed that the GFP fluorescence intensity in *nmur-1*(*ok1387*) animals was stronger than that seen in wild-type animals (Figure 2A). Intestinal bacterial loads were quantified by counting the colony-forming units (CFU) of live bacterial cells recovered from the intestine. The mutant animals had more *E. faecalis* CFU than wild-type animals (Figure 2B). These results indicated that the *nmur*-1 mutation caused increased intestinal accumulation of *E. faecalis*. Such higher bacterial accumulation could be due to altered pathogen intake, expulsion, or clearance by immunity. These possible causes were further investigated. *C. elegans* feeds on bacterial food via rhythmic contractions (pumping) of its pharynx. To determine whether there were any differences in pathogen intake between wild-type and *nmur-1*(*ok1387*) animals, we measured their pharyngeal pumping rates on bacterial lawns. When feeding on *E. faecalis*, both wild-type and mutant animals showed similar pumping rates, reflecting similar levels of pathogen intake (Figure 2C). Bacterial evacuation was assessed by measuring the defecation rate, defined as the time interval between expulsions of gut contents. We found that the defecation rate of *nmur-1*(*ok1387*) animals on *E. faecalis* was comparable with the rate observed in wild-type animals (Figure 2D). Overall, these results indicate that the reduced survival of *nmur-1*(*ok1387*) animals exposed to *E. faecalis* is likely due to increased pathogen accumulation in the intestine. Because the *nmur-1* mutation did not alter *E. faecalis* intake or expulsion, the increased pathogen accumulation likely resulted from the mutants' weakened innate immunity that was unable to clear the infection from the intestine.

We next performed similar experiments to investigate intestinal accumulation, intake, and expulsion of *S. enterica*. Our results showed that, compared with wild-type animals, *nmur-1*(*ok1387*) animals exhibited slightly weaker GFP-tagged *S. enterica* fluorescence intensities (Figure 2E) and had significantly lower CFU counts (Figure 2F), indicating that the *nmur*-1 mutation decreased intestinal accumulation of *S. enterica*. Mutant animals also had slightly higher pharyngeal pumping rates than wild-type animals (Figure 2G), suggesting that pathogen intake was increased in the mutants despite their reduced bacterial accumulation. The defecation rate of *nmur-1*(*ok1387*) animals on *S. enterica* was comparable with that of wild-type animals (Figure 2H). These results indicate that the enhanced survival of *nmur-1*(*ok1387*) animals exposed to *S. enterica* is likely due to decreased pathogen accumulation in the intestine. This decrease did not result from reduced pathogen intake (pathogen intake actually enhanced) or increased expulsion but likely resulted from enhanced innate immunity in the mutants that cleared the infection

from the intestine. Taken together, both the *E. faecalis* and *S. enterica* studies suggest that NMUR-1 could regulate innate immunity in *C. elegans* defense against pathogen infection but plays opposite roles in such potential regulation against the two pathogens.

NMUR-1 regulates *C. elegans* transcriptional activity

To gain insights into how NMUR-1 regulates *C. elegans* defense at the molecular level, we employed RNA sequencing (RNA-seq) to profile gene expression in wild-type and *nmur-1*(*ok1387*) animals with or without pathogen infection. We first compared the gene expression profiles of *nmur-1*(*ok1387*) animals with those of wild-type animals under normal conditions (i.e., without infection). In total, 14,206 genes were detected and quantified with a false discovery rate (FDR) of 5%. Among these genes, 1,599 were upregulated and 275 were downregulated at least 2-fold in *nmur-1*(*ok1387*) animals relative to wild-type animals. The change in expression of such a large number of genes in the mutant worms indicates that the lack of NMUR-1 profoundly affects gene expression in *C. elegans*. Gene ontology (GO) analysis of the 1,599 upregulated genes identified 26 significantly enriched molecular functions, including protein kinase/phosphatase activity, ribonucleotide binding, and cuticle structure activity (Table S1). Interestingly, GO analysis of the 276 downregulated genes showed 11 significantly attenuated molecular functions, all of which involve transcription-related DNA-binding activities (Table 1, “Attenuated molecular functions without exposure to pathogens”). Twenty-three downregulated genes possess these activities and contribute to the functional attenuation, most of which encode transcription factors involved in binding to RNA polymerase II regulatory regions (Table 2, “Downregulated genes related to the attenuated molecular functions without exposure to pathogens”). These results indicate that NMUR-1 could affect transcription by regulating the expression of these transcription factors.

Because of the high importance of transcription in the fundamental functions of life and the potential regulatory role of NMUR-1 in this process, we next examined how NMUR-1, or the lack thereof, impacts transcription. To this end, we developed an *in vitro* transcription system to measure *C. elegans* transcriptional activity (Wibisono et al., 2020). One of the biggest obstacles for biochemical studies of *C. elegans* is the high difficulty of preparing functionally active nuclear extract due to its thick surrounding cuticle. In our transcription system, Balch homogenization was employed to effectively disrupt worms, and functionally active nuclear extracts were obtained through subcellular fractionation. Subsequently, the nuclear extracts were used to reconstitute *in vitro* transcription reactions with a linear DNA template containing the worm *Δpes-10* promoter, followed by PCR-based, non-radioactive detection of transcripts (Wibisono et al., 2020). Using this system, we were able to compare the general transcriptional activity of *nmur-1*(*ok1387*) animals with that of wild-type animals at the whole-organism level. PCR and gel analysis of the transcript products showed substantial increases in transcriptional activity in reactions with mutant nuclear extract compared with those with wild-type nuclear extract (Figure 3A). To quantitatively compare the transcriptional activity of wild-type and mutant nuclear extracts, we next titrated the DNA template with varying amounts of each extract and used qRT-PCR to quantify transcripts at each titration point. The resulting data were then fitted with the Michaelis-Menten model and the non-linear least-squares method, as

we described previously (Wibisono et al., 2020). The titration curves and two titration parameters, namely, the maximum yield and the amount of nuclear extract needed to reach 50% of the maximum yield, are shown in Figure 3B. Compared with the titrations with wild-type nuclear extract, those with mutant extract yielded 2.33-fold maximum number of transcripts and only needed 0.67-fold extract to reach 50% of the maximum yield (Figure 3B), indicating that the reactions performed with mutant extract were more robust and had higher transcriptional activity. These results were surprising given the fact that the expression of many transcription factors was downregulated in the mutant animals. Taken together, our data suggest that NMUR-1 suppresses transcriptional activity in wild-type animals and that functional loss of NMUR-1 abrogates this suppression, which explains why a large number of genes (1,599 genes) were upregulated in *nmur-1*(*ok1387*) animals relative to wild-type animals.

We also employed *in vivo* transcription assays to evaluate how the lack of NMUR-1 affects transcriptional activity in *C. elegans*. For these assays, transgenic strain CL2070, which contains the *hsp-16.2p*::*GFP* reporter transgene, was used. This strain does not express detectable GFP under standard conditions but broadly expresses GFP in all tissues after heat shock, allowing for the assessment of overall transcriptional activity in living animals (Link et al., 1999). The CL2070 animals were outcrossed with our wild-type animals and then crossed with *nmur-1*(*ok1387*) animals. The resulting animals (*CL2070*(*dvIs70*) and *CL2070*(*dvIs70*);*nmur-1*(*ok1387*)) were grown to the L4 larval stage, heat shocked at 35°C for 2 h, and returned to 20°C for GFP mRNA quantification by qRT-PCR. Our results showed that GFP transcription was significantly increased in *CL2070*(*dvIs70*); *nmur-1*(*ok1387*) animals compared with *CL2070*(*dvIs70*) animals (Figure 3C), indicating that the *nmur-1* mutation causes higher overall transcriptional activity, which is in agreement with the results of our *in vitro* transcription assays. Consistently, we also observed higher GFP expression at the protein level in *CL2070*(*dvIs70*);*nmur-1*(*ok1387*) animals compared with *CL2070* (*dvIs70*) animals (Figure S5). Although heat shock broadly affects gene expression (Brunquell et al., 2016; Snoek et al., 2017), little overlap was detected between genes in the heat-shock response and NMUR-1-regulated genes identified in *nmur-1*(*ok1387*) animals relative to wild-type animals by RNA-seq (Table S2), indicating that the heat-shock pathway and the NMUR-1 pathway are unrelated and that heat-shock treatment is unlikely to interfere with NMUR-1-specific effects on transcription activity.

NMUR-1 regulates the innate immune response to *E. faecalis* by controlling the expression of C-type lectins

Before investigating NMUR-1-dependent immune responses to specific pathogens, we asked whether functional loss of NMUR-1 triggers any immune response under non-infectious conditions. To address this question, we examined immune effector genes regulated in *nmur-1*(*ok1387*) animals relative to wild-type animals. In *C. elegans*, seven categories of genes encode immune effectors that have proven or putative antimicrobial activity (Kim and Ewbank, 2018; Simonsen et al., 2012). These include genes encoding the saposin-like amoebapores (SPPs), antimicrobial peptides (AMPs), defensins, lysozymes, thaumatins, proteins containing CUB or CUB-like domains, and C-type lectins and galectins. A comparison of each category of genes with NMUR-1-regulated genes yielded no significant

overlaps between the two groups (Table S3). This result indicates that NMUR-1, or the lack thereof, does not impact the expression of immune effector genes and thus does not trigger any immune effector responses. Next, we asked how NMUR-1 regulates gene expression in *C. elegans* in response to *E. faecalis* infection. By examining the gene expression profiles of *nmur-1*(*ok1387*) animals relative to wild-type animals exposed to *E. faecalis*, we found that 229 genes were upregulated and 106 genes were downregulated at least 2-fold. GO analysis of the upregulated genes identified 11 significantly enriched biological processes, all of which involve defense responses to bacteria or other external stimuli (Table S4). This is consistent with the fact that *E. faecalis* is a pathogenic agent for *C. elegans* (Yuen and Ausubel, 2018). GO analysis of the downregulated genes yielded one significantly attenuated molecular function involving carbohydrate binding activity (Table 1, "Attenuated molecular functions upon exposure to *E. faecalis*"). Fifteen of the downregulated genes were related to this activity, 14 of which encode C-type lectins (Table 2, "Downregulated genes related to the attenuated molecular functions upon exposure to *E. faecalis*"). We also performed qRT-PCR to measure the expression of five of the most downregulated C-type lectin genes (*clec-94*, *clec-137*, *clec-157*, *clec-208*, and *clec-263*) and confirmed that these genes are indeed downregulated in *nmur-1*(*ok1387*) animals relative to wild-type animals exposed to *E. faecalis* (Figure S6A), which validates the RNA-seq analysis. C-type lectins are a group of proteins that contain one or more C-type lectin-like domains and recognize complex carbohydrates on cells and tissues (Drickamer and Dodd, 1999; Takeuchi et al., 2008). C-type lectins may act in pathogen recognition or function as immune effectors to fight infection (Pees et al., 2016; Sun et al., 2016). Therefore, downregulation of C-type lectins in *nmur-1*(*ok1387*) animals might explain the reduced survival observed in mutant animals following exposure to *E. faecalis*.

To determine whether NMUR-1-regulated C-type lectin genes contribute to the reduced survival of *nmur-1*(*ok1387*) animals, we inactivated these genes using RNAi-mediated knockdown in wild-type and *nmur-1*(*ok1387*) animals and assayed for their survival against *E. faecalis*-mediated killing. Five of the most downregulated C-type lectin genes (*clec-94*, *clec-137*, *clec-157*, *clec-208*, and *clec-263*) were individually targeted in these studies. While RNAi of these genes did not further reduce the survival of *nmur-1*(*ok1387*) animals (Figure 4B), knockdown of four of the five genes (all except *clec-157*) significantly suppressed the survival of wild-type animals (Figure 4A). These results indicate that some of the NMUR-1-regulated C-type lectin genes are indeed required for *C. elegans* defense against *E. faecalis* infection.

Since knockdown of C-type lectins in wild-type animals recaptured the reduced survival phenotype of *nmur-1*(*ok1387*) animals, we next asked whether complementing the expression of these C-type lectins in mutant animals could rescue their survival phenotype. To this end, we employed transgenes to express *clec-94*, *clec-208*, and *clec-263*, respectively, in *nmur-1*(*ok1387*) and wild-type animals. Survival assays against *E. faecalis* showed that while overexpression of these C-type lectins had no effect on wild-type animal survival, the expression of *clec-94* or *clec-208* partially rescued the reduced survival of the mutant animals (Figure 4C), confirming that the downregulation of C-type lectins contributes to the reduced survival of *nmur-1* mutants challenged with *E. faecalis*.

NMUR-1 suppresses the innate immune response to *S. enterica* by inhibiting unfolded protein response genes

We also compared the gene expression profiles of *nmur-1*(*ok1387*) animals with those of wild-type animals exposed to *S. enterica* and found that 28 genes were upregulated and 28 genes were downregulated at least 2-fold. While GO analysis of the downregulated genes did not yield any attenuated GO terms, a similar analysis of the upregulated genes identified four significantly enriched biological processes and two significantly enriched molecular functions (Table 1, "Enriched biological processes and molecular functions upon exposure to *S. enterica*"). Among these enrichments, the biological process "protein quality control for misfolded or incompletely synthesized proteins" was the most significantly enriched (FDR = 7.89×10^{-5}) and has a known role in immune responses to pathogen infection (Grootjans et al., 2016). Under an environmental stress, such as pathogen infection, increased demand for protein folding causes ER stress, which activates the unfolded protein response (UPR) pathways to alleviate the stress and maintain protein homeostasis. This process is known to be controlled by the nervous system (Aballay, 2013). Four of the upregulated genes (*T20D4.3*, *T20D4.5*, *C17B7.5*, and *npl-4.2*) are related to UPR activity and contributed to the biological process enrichment (Table 2, "Upregulated genes related to the enriched biological process protein quality control upon exposure to *S. enterica*"). qRT-PCR measurements of these four genes confirmed that their expression is indeed upregulated in *nmur-1*(*ok1387*) animals relative to wild-type animals exposed to *S. enterica* (Figure S6B).

To determine whether these NMUR-1-regulated UPR genes play any roles in the enhanced survival of *nmur-1*(*ok1387*) animals, we inactivated these genes individually using RNAi and then assayed the animals for survival against *S. enterica*. Because these genes are mainly expressed in neurons (Worm-Base), we employed strain *TU3401*, which is capable of RNAi-mediated gene knockdown in neurons (Calixto et al., 2010), in our experiments. While RNAi of *npl-4.2* suppressed the survival of both TU3401 and *nmur-1*(*ok1387*);*TU3401* animals following exposure to *S. enterica*, RNAi silencing of *T20D4.3* specifically suppressed the enhanced survival of *nmur-1*(*ok1387*);*TU3401* animals (Figures 4D and 4E). In comparison, RNAi of *T20D4.5* or *C17B7.5* had no effect on animal survival (Figures 4D and 4E). The two genes that showed effects on survival, *npl-4.2* and *T20D4.3*, have known roles in the UPR. NPL-4.2 has been implicated in ER-associated protein degradation. Specifically, NPL-4 forms a complex with CDC-48 ATPase and UFD-1, which extracts polyubiquitin-tagged misfolded proteins from the ER membrane and facilitates their degradation by the proteasome (Bays et al., 2001; Ye et al., 2001). *T20D4.3* encodes a peptide N-glycanase and acts in ER-associated degradation system to surveil ER quality control/homeostasis for newly synthesized glycoproteins; it reportedly functions in longevity, dauer formation, and pathogen responses (Gaglia et al., 2012).

Because upregulation of the UPR genes in *nmur-1*(*ok1387*) animals leads to enhanced survival of the mutants, we asked whether overexpression of these genes in wild-type animals can mimic the enhanced survival phenotype. To this end, we generated transgenic strains JRS78 and JRS79 that overexpress *T20D4.3* mRNA in wild-type *N2* and *nmur-1*(*ok1387*) animals, respectively (Table S5). Survival assays against *S. enterica* showed

that overexpression of *T20D4.3* significantly improved the survival of wild-type animals but did not further increase the survival of *nmur-1* mutant animals (Figure 4F). Taken together, our results indicate that some NMUR-1-regulated UPR genes are important for *C. elegans* defense against *S. enterica*, and that NMUR-1 can suppress the innate immune response to *S. enterica* by inhibiting UPR genes.

The NMUR-1 ligand CAPA-1 is required for *C. elegans* defense against *E. faecalis* but not against *S. enterica*

CAPA-1, a homolog of vertebrate NMU and insect *capability* peptides, is an endogenous ligand of NMUR-1 (Lindemans et al., 2009; Watteyne et al., 2020). To determine whether CAPA-1 plays any roles in *C. elegans* defense, we examined the survival of a loss-of-function mutant of CAPA-1, *capa-1*(*ok3065*), after *E. faecalis* exposure. Compared with wild-type animals, *capa-1*(*ok3065*) animals showed reduced survival, a phenotype also displayed by *nmur-1*(*ok1387*) animals (Figure 5A). We then crossed *capa-1*(*ok3065*) with *nmur-1*(*ok1387*) animals to generate *capa-1*(*ok3065*);*nmur-1*(*ok1387*) double mutants. These double mutants exhibited reduced survival against *E. faecalis*, similar to *nmur-1*(*ok1387*) animals (Figure 5A). These results indicate that CAPA-1 and NMUR-1 likely function in the same pathway to mediate *C. elegans* defense against *E. faecalis*. To investigate whether CAPA-1 is a ligand of NMUR-1 in the defense response, we tested whether exogenous administration of a synthetic CAPA-1 peptide could rescue the reduced survival phenotype of the mutant animals. To this end, we exposed wild-type and mutant animals to *E. faecalis* on brain heart infusion medium containing 1 μg/mL synthetic CAPA-1 peptide and scored their survival over time. Our results showed that exogenous CAPA-1 peptide rescued the reduced survival phenotype of *capa-1*(*ok3065*) animals but failed to rescue *nmur-1*(*ok1387*) animals or *capa-1*(*ok3065*);*nmur-1*(*ok1387*) double mutants (Figure 5B). These results demonstrate that the function of NMUR-1 in defense depends on the presence of CAPA-1, and vice versa, indicating that CAPA-1/NMUR-1 function as a ligand/receptor pair in mediating *C. elegans* defense against *E. faecalis*.

To determine whether CAPA-1 also functions in the *C. elegans* defense response to *S. enterica*, we subjected wild-type and mutant animals to survival assays against *S. enterica*. Results showed that while *capa-1*(*ok3065*) animals displayed survival at the wild-type level, *capa-1*(*ok3065*);*nmur-1*(*ok1387*) double mutants exhibited survival comparable with that of *nmur-1*(*ok1387*) animals (Figure 5C). This indicates that lacking CAPA-1 has no influence on *C. elegans* defense against *S. enterica*, and that CAPA-1 might not be involved in NMUR-1-mediated innate immune response to this pathogen. To further test this notion, we exposed wild-type and mutant animals to *S. enterica* on nematode growth medium (NGM) containing 0 or 1 μg/mL synthetic CAPA-1 peptide and scored their survival over time (Figure 5D). In a parallel experiment, we first soaked wild-type and mutant animals in M9 buffer with 0 or 1 μg/mL synthetic CAPA-1 peptide for 1 h, exposed the animals to *S. enterica* on NGM plates containing 0 or 1 μg/mL CAPA-1 peptide, and scored them for survival over time (Figure S7). The results from both experiments showed that exogenous CAPA-1 peptide failed to influence the survival phenotype of *capa-1*(*ok3065*), *nmur-1*(*ok1387*), or *capa-1*(*ok3065*);*nmur-1*(*ok1387*) double mutant animals (Figures 5D and S7), confirming that CAPA-1 is neither a ligand of NMUR-1 nor required in *C. elegans*

defense against *S. enterica*. Although CAPA-1 is the only NMUR-1 ligand identified so far (Lindemans et al., 2009; Watteyne et al., 2020), these results suggest that other ligands may exist and that NMUR-1 could bind to different ligands to regulate immune responses to distinct pathogens. Such a notion is consistent with the expression patterns of CAPA-1 and NMUR-1, that is, CAPA-1 is only expressed in ASG chemosensory neurons (Lindemans et al., 2009; Watteyne et al., 2020) while NMUR-1 is more broadly expressed and thus has higher chances to interact with other ligands (NMUR-1 is expressed in the spermathecae of the somatic gonad as well as in several different types of sensory neurons [ADF, ADL, AFD, and OLQ], interneurons [AIA, AIZ, AVK, DVA, PVT, RIC, RIH, and SDQ], and some other neurons [PDA, ALA, SIB, and two other head neurons] [Maier et al., 2010; Watteyne et al., 2020]). Interestingly, by using the *nmur-1p*::*gfp* transcriptional reporter, we observed that distinct subsets of NMUR-1-expressing neurons are activated upon exposure to *E. faecalis* and *S. enterica*, respectively (Figure S8). Taken together, our study indicates that different NMUR-1-dependent neural circuits could be involved in regulating the immune responses to the two pathogens.

DISCUSSION

In the current study, we have shown that *C. elegans* lacking the neuronal GPCR NMUR-1 exhibited altered survival against various bacterial pathogens. By focusing on two pathogens, *E. faecalis* and *S. enterica*, as infecting agents, we have demonstrated that NMUR-1 regulates distinct immune responses to different pathogens. Recent behavior research in *C. elegans* indicates that its nervous system might play a major role in pathogen detection (Kim and Flavell, 2020). In this context, a relevant question would be whether neuronal NMUR-1 mediates the specificity of innate immunity by directly interacting with bacterial molecules. We have shown that NMUR-1 has diverse effects on *C. elegans* defense against various bacterial pathogens (Figures 1, S1, and S2). If the hypothesis that NMUR-1 directly interacts with pathogens is correct, this GPCR should be able to bind to various pathogen-derived molecules. Such a scenario seems unlikely given that PRR-PAMP interactions follow a simple key-lock system, i.e., each receptor matches one pathogen-associated molecule or molecular pattern (Schulenburg et al., 2007). Therefore, it is more likely that NMUR-1 mediates the ability to differentiate between pathogens by controlling neural signaling than by recognizing bacterial molecules directly. Indeed, we have found that NMUR-1 regulates C-type lectin genes in response to *E. faecalis* infection but UPR genes in response to *S. enterica* infection; both of these genes are known to function in innate immune signaling pathways that fight infection (Sun et al., 2016).

How does NMUR-1, a single type of neuronal GPCR, distinguish different pathogens so that it can respond to some attacks with suppression of the innate immune response and amplify the response to others? A basic principle in neuroscience is that the interaction of multiple neural circuits mediates the functional output of a neural network and determines the final state of organ function (Tracey, 2014). Accordingly, the net effect of neural control on the immune response depends on the total sum of the interactions resulting from ligand-receptor signal transduction in a specific path. NMUR-1 is normally expressed in the spermathecae of the somatic gonad and several different types of sensory neurons as well as in interneurons (Maier et al., 2010). By using a fluorescent reporter transgene, we observed that distinct

subsets of NMUR-1-expressing neurons are activated upon exposure to *E. faecalis* and *S. enterica* (Figure S8), indicating that different neural circuits are involved in regulating the immune responses to these two pathogens. This notion is further supported by the fact that CAPA-1, the only NMUR-1 ligand identified so far, is required for the nematode immune response to *E. faecalis* but is dispensable for its response to *S. enterica* (Figure 5). Future studies to decipher these different neuroimmune regulatory circuits would help us understand how signals pass through different components of the circuits to exert a net effect on immunity. An associative learning circuit mediated by CAPA-1/NMUR-1 signaling was recently uncovered in *C. elegans* in which sensory ASG neurons release CAPA-1, which signals via NMUR-1 in AFD sensory neurons to specifically mediate the retrieval of learned salt avoidance (Watteyne et al., 2020). In mice, cholinergic neurons in the intestine can sense and respond to infection by expressing NMU, which directly activates type 2 innate lymphoid cells in the gastrointestinal tract through NMUR1 to drive anti-parasitic immunity (Cardoso et al., 2017; Klose et al., 2017; Wallrapp et al., 2017). These studies provide useful information for deciphering NMUR-1-mediated neuroimmune regulatory circuits in *C. elegans*, which will be critical for further understanding how the nervous system regulates innate immunity to generate specificity by either suppressing or amplifying immune responses to different pathogens.

Limitations of the study

In this study, we have discovered that neuronal GPCR NMUR-1 regulates distinct immune responses to different pathogens. This discovery is based on the observation that functional loss of NMUR-1 had diverse effects on *C. elegans* innate immunity against six bacterial pathogens and two *E. coli* strains. The effects of NMUR-1 on immunity against other pathogens have not been explored. The molecular mechanism underlying NMUR-1-mediated regulation, i.e., NMUR-1 modulates *C. elegans* transcriptional activity that controls the expression of distinct immune genes in response to different pathogens, is derived from the analyses of infections with two pathogens, namely, *E. faecalis* and *S. enterica*. The molecular details of infections with other pathogens have not been examined. The NMUR-1-expressing neurons that are activated upon exposure to *E. faecalis* or *S. enterica* were identified by analyzing cell position and axon structure, but the neuronal identities have not been experimentally confirmed.

STAR★METHODS

RESOURCE AVAILABILITY

Lead contact—Information and request regarding resources and reagents should be directed to and will be fulfilled by the lead contact, Jingru Sun (Jingru.sun@wsu.edu)

Materials availability—The *C. elegans* strains and recombinant DNA generated in this study will be shared upon request, but we may require payment to cover shipment and completion of a Material Transfer Agreement for possible commercial applications.

Data and code availability

- The raw RNA sequence data (FASTQ files) were deposited in NCBI's SRA database through the GEO. The processed gene quantification files and differential expression files were deposited in GEO. All of these data can be accessed through GEO with the accession number GEO: GSE154324.
- No original code was created during the course of this study.
- Any additional information required to reanalyze the data reported in this paper is available from the lead contact upon request.

EXPERIMENTAL MODEL AND SUBJECT DETAILS

Nematode strains—The following *C. elegans* strains were maintained as hermaphrodites at 20°C, grown on modified Nematode Growth Media (NGM) (0.35% instead of 0.25% peptone) with 30 units/mL nystatin and 15 μg/mL tetracycline, and fed *E. coli* HT115. The wild-type animal strain was *C. elegans* Bristol *N2*. The *capa-1*(*ok3065*), *CL2070*(*dvls70*), and *TU3401* strains were obtained from the *Caenorhabditis* Genetics Center (University of Minnesota, Minneapolis, MN). *nmur-1*(*ok1387*) and *nmur-1p*::*gfp* animals used in this study were gifts from Dr. Joy Alcedo (Wayne State University, Detroit, MI). The *capa-1*(*ok3065*);*nmur-1*(*ok1387*), *nmur-1*(*ok1387*);*CL2070*(*dvls70*), and *nmur-1*(*ok1387*);*TU3401* mutant strains were constructed using standard genetic techniques. *nmur-1*(*its1672*) animals were generated using a common CRISPR/Cas9 genome editing protocol (Watteyne et al., 2020). All mutant animals were backcrossed with wild-type Bristol *N2* animals at least three times before experimental use. All genotypes were confirmed using PCR or sequencing. All *C. elegans* animals used for this study were synchronized 65-hour old young adults unless otherwise noted in the specific methodology.

Bacterial strains—The following bacterial strains were grown using standard conditions (Lagier et al., 2015): *Escherichia coli* HT115, *Escherichia coli* OP50, *Salmonella enterica* strain SL1344, *S. enterica SL1344*::*gfp*, *Pseudomonas aeruginosa* strain PA14, *Yersinia pestis* strain KIM5, *Enterococcus faecalis* strain OG1RF, *E. faecalis OG1RF*::*gfp*, *Microbacterium nematophilum* strain CBX102, and *Staphylococcus aureus* strain MSSA476.

METHOD DETAILS

Survival assay—Wild-type and mutant animals were synchronized by egg-laying. Briefly, well-fed gravid adult animals were transferred to fresh *E. coli* HT115 seeded NGM plates and incubated for 45 minutes at 25°C. Adult animals were removed after 45 minutes, and the synchronized offspring were grown at 20°C for 65 hours. Bacterial lawns for the survival assays were prepared by culturing pathogenic bacteria for 15~16 hours in either Luria broth (LB) or brain heart infusion (BHI) broth for *E. faecalis* OG1RF at 37°C in a shaking incubator. A 30 μL drop of the fresh bacterial culture was placed on 3.5 cm plates of either modified NGM or BHI media with 10 μg/mL of gentamycin. Full-lawn survival assays were prepared by spreading the 30 μL of bacterial culture over the complete surface of each 3.5 cm plate. Plates were incubated at 37°C for 15~16 hours, cooled to room temperature, and then seeded with synchronized 65-hour-old young adult animals. The survival assays were

performed at 25°C, and live animals were transferred daily to fresh plates until egg laying ceased. Animals were scored at the times indicated and were considered dead when they failed to respond to touch.

Lawn occupancy assay—Synchronized 65-hour-old animals and bacteria plates were prepared using the method described above. Synchronized animals were placed in the center of the bacterial lawn and allows to crawl freely on the plate. The number of animals on the bacteria lawn were counted at 4-, 8-, 12-, 24-, and 36-hours post-exposure. The assays were performed at 25°C and dead animals were censored. The results were calculated as a percentage of animals on the bacteria lawn versus the total number of animals on the plates at the given time point.

Profiling bacterial accumulation in the nematode intestine—Synchronized 65-hour-old animals were prepared using the method describe above. GFP-tagged bacteria were prepared using the method described above with the addition of selective antibiotics (*S. enterica* SL1344::*gfp* – 50 μg/mL of kanamycin; *E. faecalis* OG1RF::*gfp* – 100 μg/mL rifampicin) in the media plates. Synchronized animals were transferred to the plates seeded with GFP-tagged bacteria and incubated for 24 hours at 25°C. Following incubation, the animals were transferred to an empty NGM plate for 15 minutes to eliminate any fluorescent bacteria stuck to the body. The animals were then transferred to a new, empty NGM plate and into a droplet of M9 buffer to further wash away any bacteria remaining on the body. Animals were anesthetized using 25 mM Sodium Azide and placed on a 2% agarose pad. A drop of halocarbon oil was placed over the anesthetized animals to minimize bubbles and other artifacts before being covered with a glass coverslip. The animals were visualized using a Zeiss Axio Imager M2 stereoscopic microscope.

Quantification of intestinal colonization—Synchronized 65-hour-old animals were prepared using the method describe above. GFP-tagged bacteria were prepared using the method described above with the addition of antibiotics in the media plates. Synchronized animals were transferred to the plates seeded with GFP-tagged bacteria and incubated for 24 hours at 25°C. Ten animals were transferred to a 1.5 mL tube containing a solution of 25 mM Sodium Azide with 1 mg/mL ampicillin and tetracycline. The animals were then soaked for 45 minutes to remove any external bacteria. After 45 minutes, the animals were washed three times with PBS containing 0.1% Triton X-100 to remove the remaining antibiotics, and ground in 100 μL of PBS with 0.1% Triton. Serial dilutions of the lysates (10^{-1}, 10^{-2}, 10^{-3}, 10^{-4}, and 10^{-5}) were plated with kanamycin or rifampicin to select for GFP-tagged bacteria and the plates were incubated at 37°C for 24 hours.

Profiling pumping and defecation rates—Synchronized 65-hour-old animals, and bacteria plates were prepared using the method described above. Synchronized animals were transferred to plates seeded with pathogenic bacteria and incubated for 24 hours at 25°C. Pumping rates were counted by observing the contraction/relaxation cycles of the terminal pharyngeal bulb using a stereoscopic microscope. Cycles were counted for 30 second durations, three times for ten individual animals per condition. Defecation rates were measured by timing the span between the contraction of the rectal muscles and subsequent

excretion using a stereoscopic microscope. Cycles were counted five times for ten individual animals per condition.

RNAi interference—RNAi was conducted using the Ahringer group library and feeding synchronized L3 larval *C. elegans E. coli* strain HT115(DE3) expressing double-stranded RNA (dsRNA) that was homologous to a target gene (Fraser et al., 2000; Timmons and Fire, 1998). Before exposure, all RNAi clone plasmids were isolated, digested with KpnI, and Sanger sequenced using a T7 promoter primer to check for gene specificity. *E. coli* with the appropriate dsRNA vector were grown in LB broth containing ampicillin (100 μg/mL) at 37°C for 15–16 hours and 120 μL was plated on modified NGM plates containing 100 μg/mL ampicillin and 3 mM isopropyl β-D-thiogalactoside (IPTG). The bacteria were allowed to grow for 15–16 hours at 37°C. The plates were cooled away from direct light before the synchronized L3 larval animals were placed on the bacteria. The animals were incubated at 20°C for 24 hours or until the animals were 65 hours old. *unc-22* RNAi was included as a positive control in all experiments to account for RNAi efficiency.

Synthetic NMUR-1 ligand administration—Synchronized 65-hour-old animals, and bacteria plates were prepared using the method described above. Synchronized animals were transferred to modified NGM or BHI bacteria plates containing 0, 1, or 5 μg/mL oligopeptide AFFYTPRI-NH2. The survival assays were performed at 25°C and live animals were transferred daily to fresh plates until egg laying ceased. The animals were scored at the times indicated and were considered dead when they failed to respond to touch.

Wild-type and mutant animals were also lysed using a solution of sodium hydroxide and bleach (ratio 5:2), washed, and eggs were synchronized for 22 hours in S-basal liquid medium at room temperature. Synchronized L1 larval animals were transferred onto modified NGM plates seeded with *E. coli* HT115 and grown at 20°C for 65 hours. Synchronized animals were washed in M9 buffer and soaked for one hour in M9 buffer containing 0, 1, or 5 μg/mL oligopeptide AFFYTPRI-NH2. Soaked animals were transferred to modified NGM medium containing 0, 1, or 5 μg/mL oligopeptide AFFYTPRI-NH2 seeded with 30 μL of fresh pathogen culture that was incubated at 37°C for 15–16 hours. The survival assays were performed at 25°C and live animals were transferred daily to fresh plates until egg laying ceased. The animals were scored at the times indicated and were considered dead when they failed to respond to touch.

RNA isolation—Gravid adult wild-type and *nmur-1*(*ok1387*) animals were lysed using a solution of sodium hydroxide and bleach (ratio 5:2), washed, and eggs were synchronized for 22 hours in S-basal liquid medium at room temperature. Synchronized L1 larval animals were transferred onto modified NGM plates seeded with *E. coli* HT115 and grown at 20°C for 48 hours until the animals had reached the L4 larval stage. The animals were collected and washed with M9 buffer before being transferred to plates containing *E. coli* HT115 or pathogenic bacteria for 24 hours at 25°C. After 24 hours, animals were collected and washed with M9 buffer. RNA was extracted using QIAzol (Qiagen) and the RNeasy plus mini kit (Qiagen) following the protocol provided by the manufacturer.

Quantitative real-time PCR (qRT-PCR)—Total RNA was obtained as described above. 2 μg of RNA were used to generate cDNA in a 100 μL reaction using the Applied Biosystems High-Capacity cDNA Reverse Transcription Kit. qRT-PCR was conducted by following the prescribed protocol for PowerUp SYBR Green (Applied Biosystems) on an Applied Biosystems StepOnePlus real-time PCR machine. 10 μL reactions were set up following the manufacturer's recommendations, and 20 ng of cDNA was used per reaction. Relative fold-changes for transcripts were calculated using the comparative $C_T (2^{-\Delta\Delta CT})$ method and were normalized to pan-actin (*act-1, -3, -4*). Amplification cycle thresholds were determined by the StepOnePlus software. All samples were run in triplicate. Primer sequences are available in Table S6.

RNA sequencing—Total RNA samples were obtained as described above and was submitted to the WSU Genomics Core for RNA-seq analyses. RNA-seq and related bioinformatic analyses were done following our published protocol (Sellegounder et al., 2019).

In vitro* transcription assay—In vitro* transcription assays were performed following our published protocol (Wibisono et al., 2020). Briefly, nuclear extracts were prepared from synchronized young adult animals using Balch homogenization. The nuclear extracts were then incubated with PESDNA (a linear DNA template containing the worm *Δpes-10* promoter) and other transcription components at 30°C for 30 minutes, followed by RNA purification and reverse transcription. The resulting cDNA was either amplified by PCR and detected by gel electrophoresis or quantified by qRT-PCR using the PowerUp SYBR green qPCR kit (Applied Biosystems, catalog # A25918).

In vivo* transcription quantification—CL2070*(*dvIs70*) and *nmur-1*(*ok1387*);*CL2070*(*dvIs70*) animals were synchronized as previously mentioned for RNA isolation. Synchronized L1 larval animals were transferred onto modified NGM plates seeded with *E. coli* HT115 and grown at 20°C for 48 hours until the animals had reached the L4 larval stage. The animals were collected and washed with M9 buffer before being transferred to NGM plates seeded with *E. coli* HT115 that were preheated to 35°C. Animals were then placed into a 35°C incubator for 2 hours. After the 2-hour incubation at 35°C, the animals were immediately collected and washed with M9 buffer, and snap frozen. RNA was extracted using QIAzol (Qiagen) and the RNeasy plus mini kit (Qiagen) following the protocol provided by the manufacturer. following the protocol provided by the manufacturer. RNA was reversed transcribed using 2 μg of total RNA to generate cDNA in a 100 μL reaction using the Applied Biosystems High-Capacity cDNA Reverse Transcription Kit. GFP transcripts were quantified via rt-qPCR using the PowerUp SYBR green qPCR kit (Applied Biosystems, catalog # A25918).

Visualizing heat-shock GFP expression—*CL2070*(*dvIs70*) and *nmur-1*(*ok1387*);*CL2070*(*dvIs70*) animals were synchronized as previously mentioned for RNA isolation. Synchronized L1 larval animals were transferred onto modified NGM plates seeded with *E. coli* HT115 and grown at 20°C for 48 hours until the animals had reached the L4 larval stage. The animals were collected and washed with M9 buffer before being

transferred to NGM plates seeded with *E. coli* HT115 that were preheated to 35°C. Animals were then placed into a 35°C incubator for 2 hours. After the 2-hour incubation at 35°C, the animals were transferred to a 20°C incubator and allowed to recover for 2 hours. Animals were anesthetized using 25 mM Sodium Azide and placed on a fresh 2% agarose pad. A drop of halocarbon oil was placed over the anesthetized animals to minimize bubbles and other artifacts before being covered with a glass coverslip. The animals were visualized using a Zeiss Axio Imager M2 stereoscopic microscope. GFP quantification was performed using ImageJ, individual animal GFP expression were measured for the mean gray-value. An unoccupied section of the agarose pad was measured for its mean gray-value to account for background fluorescence.

Plasmid construction and transgenic animal generation—A *clec-94* genomic DNA fragment (4,247 bp) was amplified by PCR from mixed stage wild-type *C. elegans* using the following primers: 5′-ATTGTCGACGTACAGTCCCACTACTTGTTGC-3′ and 5′-CTAGGATCCCTAACATTGGCCGGGAAAGAG-3′. PCR products were then cloned into the *pPD95.77* vector (Fire Lab *C. elegans* vector kit; Addgene, Cambridge, MA) via the *SalI* and *BamHI* sites. The resulting plasmid pPW01 (*clec-94p*::*clec-94*::*SL2*::*gfp*) was microinjected into wild-type animals at 10 ng/μL to generate strain JRS60 (Table S5). The *clec-94* genomic rescue strain JRS63 (Table S5) was generated by crossing JRS60 with *nmur-1*(*ok1387*) animals.

A *clec-208* genomic DNA fragment (3,556 bp) was amplified by PCR from mixed stage wild-type *C. elegans* using the following primers: 5′-TTTGTCGACTTTCTGTTCTTGCTACTCTCTACC-3′ and 5′-TTTTCTAGACTGGCTCGTTCTTAGAGACC-3′. PCR products were then cloned into the *pPD95.77* vector via the *SalI* and *XbaI* sites. The resulting plasmid, pPW02 (*clec-208p*::*clec-208*::*SL2*::*gfp*), was microinjected into wild-type animals at 50 ng/μL with *unc-122p*::*mCherry* at 20 ng/μl as a co-injection marker to generate strain JRS61 (Table S5). The *clec-208* genomic rescue strain JRS64 (Table S5) was generated by crossing JRS61 with *nmur-1*(*ok1387*) animals.

A *clec-263* genomic DNA fragment (5,389 bp) was amplified by PCR from mixed stage wild-type *C. elegans* using the following primers: 5′-TTTGTCGACGCGATGGGTGGTTGTATTATTC-3′ and 5′-CAAGGATCCAAATCGTATTTCCGTCGTTGGTC-3′. PCR products were then cloned into the *pPD95.77* vector via the *SalI* and *BamHI* sites. The resulting plasmid, pPW03 (*clec-263p*::*clec-263*::*SL2*::*gfp*), was microinjected into wild-type animals at 30 ng/μL with *unc-122p*::*mCherry* at 20 ng/μl as a co-injection marker to generate strain JRS62 (Table S5). The *clec-263* genomic rescue strain JRS65 (Table S5) was generated by crossing JRS62 with *nmur-1*(*ok1387*) animals.

A *T20D4.3* genomic DNA fragment (7,665 bp) was amplified by PCR from mixed stage wild-type *C. elegans* using oligonucleotides 5′-GTACTGCAGCTGTGTCGCCAGAATGATTG-3′ and 5′-GATTGGCCATGTGAATGTTAAGAAGGCGTG-3′. PCR products were then cloned into vector pPD95.77 (Fire Lab *C. elegans* vector kit; Addgene, Cambridge, MA) via the

SalI and *BamHI* sites. The resulting plasmid, pPW04 (*T20D4.3p*::*T20D4.3*::*SL2*::*gfp*), was microinjected into wild-type animals at 50 ng/μL with *myo-3p*::*mCherry* at 10 ng/μl as a co-injection marker to generate overexpression strain JRS78 (Table S5). The *T20D4.3* overexpression strain JRS79 (Table S5) was generated by crossing JRS78 with *nmur-1*(*ok1387*).

Fluorescence imaging—Fluorescence microscopy was performed using synchronized *C. elegans* and imaging was captured a Zeiss Axio Imager M2 fluorescence stereomicroscope equipped with DIC and Zen 2 software. Before imaging, animals were anesthetized using 25 mM Sodium Azide and placed on a fresh 2% agarose pad. A drop of halocarbon oil was placed over the anesthetized animals to minimize bubbles and other artifacts before being covered with a 1-mm glass coverslip.

QUANTIFICATION AND STATISTICAL ANALYSIS

Survival curves were plotted using GraphPad PRISM (version 9) computer software. Survival was considered different from the appropriate control indicated in the main text when $p < 0.05$. PRISM uses the product limit or Kaplan-Meier method to calculate survival fractions and the log rank test, which is equivalent to the Mantel-Haenszel test, to compare survival curves. Occupancy assays, CFU assays, GFP fluorescence, and qRT-PCR results were analyzed using two-sample t tests for independent samples; p values < 0.05 are considered significant. All experiments were repeated at least three times, unless otherwise indicated. Statistical details for each figure are listed in its corresponding figure legend.

Supplementary Material

Refer to Web version on PubMed Central for supplementary material.

ACKNOWLEDGMENTS

We thank Dr. Danielle Garsin at the University of Texas Health Science Center, Houston for providing us with the *E. faecalis OG1RF*::*gfp* strain. We thank Dr. Joy Alcedo at Wayne State University for constructive discussions and for providing us with *N2*, *nmur-1*(*ok1387*), and *nmur-1p*::*gfp* worm strains. Some worm strains were provided by the *Caenorhabditis* Genetics Center, which is funded by the NIH Office of Research Infrastructure Programs (P40 OD010440). This work was supported by NIH (R35GM124678 to J.S.), Department of Translational Medicine and Physiology, Elson S. Floyd College of Medicine, WSU-Spokane (startup to Y.L.), and Research Foundation Flanders (G093419N to I.B.). The funders had no role in study design, data collection and interpretation, or the decision to submit the work for publication. The graphical abstract was created with BioRender.com.

REFERENCES

Aballay A (2013). Role of the nervous system in the control of proteostasis during innate immune activation: insights from *C. elegans*. PLoS Pathog. 9, e1003433. 10.1371/journal.ppat.1003433. [PubMed: 23950707]

Aballay A, Yorgey P, and Ausubel FM (2000). *Salmonella typhimurium* proliferates and establishes a persistent infection in the intestine of *Caenorhabditis elegans*. Curr. Biol 10, 1539–1542. [PubMed: 11114525]

Anyanful A, Easley KA, Benian GM, and Kalman D (2009). Conditioning protects *C. elegans* from lethal effects of enteropathogenic *E. coli* by activating genes that regulate lifespan and innate immunity. Cell Host Microbe 5, 450–462. 10.1016/j.chom.2009.04.012. [PubMed: 19454349]

Bays NW, Wilhovsky SK, Goradia A, Hodgkiss-Harlow K, and Hampton RY (2001). HRD4/NPL4 is required for the proteasomal processing of ubiquitinated ER proteins. Mol. Biol. Cell 12, 4114–4128. 10.1091/mbc.12.12.4114. [PubMed: 11739805]

Brenner S (1974). The genetics of *Caenorhabditis elegans*. Genetics 77, 71–94. [PubMed: 4366476]

Brunquell J, Morris S, Lu Y, Cheng F, and Westerheide SD (2016). The genome-wide role of HSF-1 in the regulation of gene expression in *Caenorhabditis elegans*. BMC Genomics 17, 559. 10.1186/s12864-016-2837-5. [PubMed: 27496166]

Calixto A, Chelur D, Topalidou I, Chen X, and Chalfie M (2010). Enhanced neuronal RNAi in *C. elegans* using SID-1. Nat. Methods 7, 554–559. 10.1038/nmeth.1463. [PubMed: 20512143]

Cardoso V, Chesne J, Ribeiro H, Garcia-Cassani B, Carvalho T, Bouchery T, Shah K, Barbosa-Morais NL, Harris N, and Veiga-Fernandes H (2017). Neuronal regulation of type 2 innate lymphoid cells via neuromedin U. Nature 549, 277–281. 10.1038/nature23469. [PubMed: 28869974]

Cherry S, and Silverman N (2006). Host-pathogen interactions in Drosophila: new tricks from an old friend. Nat. Immunol 7, 911–917. 10.1038/ni1388. [PubMed: 16924255]

Debroy S, van der Hoeven R, Singh KV, Gao P, Harvey BR, Murray BE, and Garsin DA (2012). Development of a genomic site for gene integration and expression in *Enterococcus faecalis*. J. Microbiol. Methods 90, 1–8. 10.1016/j.mimet.2012.04.011. [PubMed: 22542850]

Drickamer K, and Dodd RB (1999). C-Type lectin-like domains in *Caenorhabditis elegans*: predictions from the complete genome sequence. Glycobiology 9, 1357–1369. [PubMed: 10561461]

Dunny GM, Brown BL, and Clewell DB (1978). Induced cell aggregation and mating in Streptococcus faecalis: evidence for a bacterial sex pheromone. Proc. Natl. Acad. Sci. U S A 75, 3479–3483. 10.1073/pnas.75.7.3479. [PubMed: 98769]

Fraser AG, Kamath RS, Zipperlen P, Martinez-Campos M, Sohrmann M, and Ahringer J (2000). Functional genomic analysis of *C. elegans* chromosome I by systematic RNA interference. Nature 408, 325–330. 10.1038/35042517. [PubMed: 11099033]

Fuhrman LE, Goel AK, Smith J, Shianna KV, and Aballay A (2009). Nucleolar proteins suppress Caenorhabditis elegans innate immunity by inhibiting p53/CEP-1. PLoS Genet. 5, e1000657. 10.1371/journal.pgen.1000657. [PubMed: 19763173]

Gaglia MM, Jeong DE, Ryu EA, Lee D, Kenyon C, and Lee SJ (2012). Genes that act downstream of sensory neurons to influence longevity, dauer formation, and pathogen responses in *Caenorhabditis elegans*. PLoS Genet. 8, e1003133. 10.1371/journal.pgen.1003133. [PubMed: 23284299]

Grootjans J, Kaser A, Kaufman RJ, and Blumberg RS (2016). The unfolded protein response in immunity and inflammation. Nat. Rev. Immunol 16, 469–484. 10.1038/nri.2016.62. [PubMed: 27346803]

Holden MT, Feil EJ, Lindsay JA, Peacock SJ, Day NP, Enright MC, Foster TJ, Moore CE, Hurst L, Atkin R, et al. (2004). Complete genomes of two clinical *Staphylococcus aureus* strains: evidence for the rapid evolution of virulence and drug resistance. Proc. Natl. Acad. Sci. U S A 101, 9786–9791. 10.1073/pnas.0402521101. [PubMed: 15213324]

Irazoqui JE, Troemel ER, Feinbaum RL, Luhachack LG, Cezairliyan BO, and Ausubel FM (2010). Distinct pathogenesis and host responses during infection of *C. elegans* by *P. aeruginosa* and *S. aureus*. PLoS Pathog. 6, e1000982. 10.1371/journal.ppat.1000982. [PubMed: 20617181]

Kawli T, and Tan MW (2008). Neuroendocrine signals modulate the innate immunity of *Caenorhabditis elegans* through insulin signaling. Nat. Immunol 9, 1415–1424. 10.1038/ni.1672. [PubMed: 18854822]

Kim DH, and Ewbank JJ (2018). Signaling in the innate immune response. WormBook 2018. 10.1895/wormbook.1.83.2.

Kim DH, and Flavell SW (2020). Host-microbe interactions and the behavior of *Caenorhabditis elegans*. J. Neurogenet 34, 500–509. 10.1080/01677063.2020.1802724. [PubMed: 32781873]

Klose CSN, Mahlakoiv T, Moeller JB, Rankin LC, Flamar AL, Kabata H, Monticelli LA, Moriyama S, Putzel GG, Rakhilin N, et al. (2017). The neuropeptide neuromedin U stimulates innate lymphoid cells and type 2 inflammation. Nature 549, 282–286. 10.1038/nature23676. [PubMed: 28869965]

Lagier JC, Edouard S, Pagnier I, Mediannikov O, Drancourt M, and Raoult D (2015). Current and past strategies for bacterial culture in clinical microbiology. Clin. Microbiol. Rev 28, 208–236. 10.1128/CMR.00110-14. [PubMed: 25567228]

Lindemans M, Janssen T, Husson SJ, Meelkop E, Temmerman L, Clynen E, Mertens I, and Schoofs L (2009). A neuromedin-pyrokinin-like neuropeptide signaling system in *Caenorhabditis elegans*. Biochem. Biophys. Res. Commun 379, 760–764. 10.1016/j.bbrc.2008.12.121. [PubMed: 19133232]

Link CD, Cypser JR, Johnson CJ, and Johnson TE (1999). Direct observation of stress response in *Caenorhabditis elegans* using a reporter transgene. Cell Stress Chaperones 4, 235–242. 10.1379/1466-1268(1999)004<0235:doosri>2.3.co;2. [PubMed: 10590837]

Liu Y, Sellegounder D, and Sun J (2016). Neuronal GPCR OCTR-1 regulates innate immunity by controlling protein synthesis in *Caenorhabditis elegans*. Sci. Rep 6, 36832. 10.1038/srep36832. [PubMed: 27833098]

Liu Y, and Sun J (2021). Detection of pathogens and regulation of immunity by the *C. elegans* nervous system. MBio 12, e02301–20. 10.1128/mbio.02301-20. [PubMed: 33785621]

Maier W, Adilov B, Regenass M, and Alcedo J (2010). A neuromedin U receptor acts with the sensory system to modulate food type-dependent effects on *C. elegans* lifespan. PLoS Biol. 8, e1000376. 10.1371/journal.pbio.1000376. [PubMed: 20520844]

Martinez VG, and O'Driscoll L (2015). Neuromedin U: a multifunctional neuropeptide with pleiotropic roles. Clin. Chem 61, 471–482. 10.1373/clinchem.2014.231753. [PubMed: 25605682]

Mazgaeen L, and Gurung P (2020). Recent advances in lipopolysaccharide recognition systems. Int. J. Mol. Sci 21, 379. 10.3390/ijms21020379.

Meisel JD, and Kim DH (2014). Behavioral avoidance of pathogenic bacteria by *Caenorhabditis elegans*. Trends Immunol. 35, 465–470. 10.1016/j.it.2014.08.008. [PubMed: 25240986]

Milling S (2019). Sophisticated specificity in the innate immune response. Immunology 158, 61–62. 10.1111/imm.13112. [PubMed: 31515802]

Pees B, Yang W, Zarate-Potes A, Schulenburg H, and Dierking K (2016). High innate immune specificity through diversified C-type lectin-like domain proteins in invertebrates. J. Innate Immun 8, 129–142. 10.1159/000441475. [PubMed: 26580547]

Peterson JW (1996). Bacterial pathogenesis. In Medical Microbiology, Baron S, ed. (University of Texas Medical Branch).

Pradel E, Zhang Y, Pujol N, Matsuyama T, Bargmann CI, and Ewbank JJ (2007). Detection and avoidance of a natural product from the pathogenic bacterium *Serratia marcescens* by *Caenorhabditis elegans*. Proc. Natl. Acad. Sci. U S A 104, 2295–2300. 10.1073/pnas.0610281104. [PubMed: 17267603]

Reddy KC, Andersen EC, Kruglyak L, and Kim DH (2009). A polymorphism in npr-1 is a behavioral determinant of pathogen susceptibility in *C. elegans*. Science 323, 382–384. 10.1126/science.1166527. [PubMed: 19150845]

Schulenburg H, Boehnisch C, and Michiels NK (2007). How do invertebrates generate a highly specific innate immune response? Mol. Immunol 44, 3338–3344. 10.1016/j.molimm.2007.02.019. [PubMed: 17391764]

Sellegounder D, Liu Y, Wibisono P, Chen CH, Leap D, and Sun J (2019). Neuronal GPCR NPR-8 regulates *C. elegans* defense against pathogen infection. Sci. Adv 5, eaaw4717. 10.1126/sciadv.aaw4717. [PubMed: 31799388]

Sellegounder D, Yuan CH, Wibisono P, Liu Y, and Sun J (2018). Octopaminergic signaling mediates neural regulation of innate immunity in *Caenorhabditis elegans*. MBio 9, .e01645–18. 10.1128/mBio.01645-18.

Sharrock J, and Sun JC (2020). Innate immunological memory: from plants to animals. Curr. Opin. Immunol 62, 69–78. 10.1016/j.coi.2019.12.001. [PubMed: 31931432]

Simonsen KT, Gallego SF, Faergeman NJ, and Kallipolitis BH (2012). Strength in numbers: "Omics" studies of *C. elegans* innate immunity. Virulence 3, 477–484. 10.4161/viru.21906. [PubMed: 23076279]

Snoek BL, Sterken MG, Bevers RPJ, Volkers RJM, Van't Hof A, Brenchley R, Riksen JAG, Cossins A, and Kammenga JE (2017). Contribution of trans regulatory eQTL to cryptic genetic variation in *C. elegans*. BMC Genomics 18, 500. 10.1186/s12864-017-3899-8. [PubMed: 28662696]

Steinman L (2004). Elaborate interactions between the immune and nervous systems. Nat. Immunol 5, 575–581. 10.1038/ni1078. [PubMed: 15164017]

Sternberg EM (2006). Neural regulation of innate immunity: a coordinated nonspecific host response to pathogens. Nat. Rev. Immunol 6, 318–328. 10.1038/nri1810. [PubMed: 16557263]

Styer KL, Singh V, Macosko E, Steele SE, Bargmann CI, and Aballay A (2008). Innate immunity in *Caenorhabditis elegans* is regulated by neurons expressing NPR-1/GPCR. Science 322, 460–464. 10.1126/science.1163673. [PubMed: 18801967]

Sun J, Aballay A, and Singh V (2016). Cellular responses to infections in *Caenorhabditis elegans*. Encyclopedia Cell Biol. 2, 845–852.

Sun J, Liu Y, and Aballay A (2012). Organismal regulation of XBP-1-mediated unfolded protein response during development and immune activation. EMBO Rep. 13, 855–860. 10.1038/embor.2012.100. [PubMed: 22791024]

Sun J, Singh V, Kajino-Sakamoto R, and Aballay A (2011). Neuronal GPCR controls innate immunity by regulating noncanonical unfolded protein response genes. Science 332, 729–732. 10.1126/science.1203411. [PubMed: 21474712]

Takeuchi T, Sennari R, Sugiura K, Tateno H, Hirabayashi J, and Kasai K (2008). A C-type lectin of *Caenorhabditis elegans*: its sugar-binding property revealed by glycoconjugate microarray analysis. Biochem. Biophys. Res. Commun 377, 303–306. 10.1016/j.bbrc.2008.10.001. [PubMed: 18848522]

Tan MW, Rahme LG, Sternberg JA, Tompkins RG, and Ausubel FM (1999). *Pseudomonas aeruginosa* killing of *Caenorhabditis elegans* used to identify *P. aeruginosa* virulence factors. Proc. Natl. Acad. Sci. U S A 96, 2408–2413. [PubMed: 10051655]

Tan RS, Ho B, Leung BP, and Ding JL (2014). TLR cross-talk confers specificity to innate immunity. Int. Rev. Immunol 33, 443–453. 10.3109/08830185.2014.921164. [PubMed: 24911430]

Timmons L, Court DL, and Fire A (2001). Ingestion of bacterially expressed dsRNAs can produce specific and potent genetic interference in *Caenorhabditis elegans*. Gene 263, 103–112. 10.1016/s0378-1119(00)00579-5. [PubMed: 11223248]

Timmons L, and Fire A (1998). Specific interference by ingested dsRNA. Nature 395, 854. 10.1038/27579. [PubMed: 9804418]

Tracey KJ (2014). Approaching the next revolution? Evolutionary integration of neural and immune pathogen sensing and response. Cold Spring Harb. Perspect. Biol 7, a016360. 10.1101/cshperspect.a016360. [PubMed: 25376836]

Une T, and Brubaker RR (1984). In vivo comparison of avirulent Vwa- and Pgm- or Pstr phenotypes of yersiniae. Infect. Immun 43, 895–900. [PubMed: 6365786]

Wallrapp A, Riesenfeld SJ, Burkett PR, Abdulnour RE, Nyman J, Dionne D, Hofree M, Cuoco MS, Rodman C, Farouq D, et al. (2017). The neuropeptide NMU amplifies ILC2-driven allergic lung inflammation. Nature 549, 351–356. 10.1038/nature24029. [PubMed: 28902842]

Watteyne J, Peymen K, Van der Auwera P, Borghgraef C, Vandewyer E, Van Damme S, Rutten I, Lammertyn J, Jelier R, Schoofs L, and Beets I (2020). Neuromedin U signaling regulates retrieval of learned salt avoidance in a *C. elegans* gustatory circuit. Nat. Commun 11, 2076. 10.1038/s41467-020-15964-9. [PubMed: 32350283]

Wibisono P, Liu Y, and Sun J (2020). A novel in vitro *Caenorhabditis elegans* transcription system. BMC Mol. Cell Biol 21, 87. 10.1186/s12860-020-00332-8. [PubMed: 33256604]

Wong D, Bazopoulou D, Pujol N, Tavernarakis N, and Ewbank JJ (2007). Genome-wide investigation reveals pathogen-specific and shared signatures in the response of *Caenorhabditis elegans* to infection. Genome Biol. 8, R194. 10.1186/gb-2007-8-9-r194. [PubMed: 17875205]

Ye Y, Liang Z, and Xue L (2021). Neuromedin U: potential roles in immunity and inflammation. Immunology 162, 17–29. 10.1111/imm.13257. [PubMed: 32888314]

Ye Y, Meyer HH, and Rapoport TA (2001). The AAA ATPase Cdc48/p97 and its partners transport proteins from the ER into the cytosol. Nature 414, 652–656. 10.1038/414652a. [PubMed: 11740563]

Yuen GJ, and Ausubel FM (2018). Both live and dead Enterococci activate *Caenorhabditis elegans* host defense via immune and stress pathways. Virulence 9, 683–699. 10.1080/21505594.2018.1438025. [PubMed: 29436902]

Zarate-Potes A, Yang W, Pees B, Schalkowski R, Segler P, Andresen B, Haase D, Nakad R, Rosenstiel P, Tetreau G, et al. (2020). The *C. elegans* GATA transcription factor elt-2 mediates distinct

transcriptional responses and opposite infection outcomes towards different *Bacillus thuringiensis* strains. PLoS Pathog. 16, e1008826. 10.1371/journal.ppat.1008826. [PubMed: 32970778]

Zhang Y, Lu H, and Bargmann CI (2005). Pathogenic bacteria induce aversive olfactory learning in *Caenorhabditis elegans*. Nature 438, 179–184. 10.1038/nature04216. [PubMed: 16281027]

Highlights

- Functional loss of NMUR-1 has diverse effects on innate immunity against pathogens
- NMUR-1 modulates transcription activity by regulating transcription factors
- NMUR-1 mediates distinct immune gene expression in response to different pathogens
- Immune specificity might be regulated by different NMUR-1-dependent neural circuits

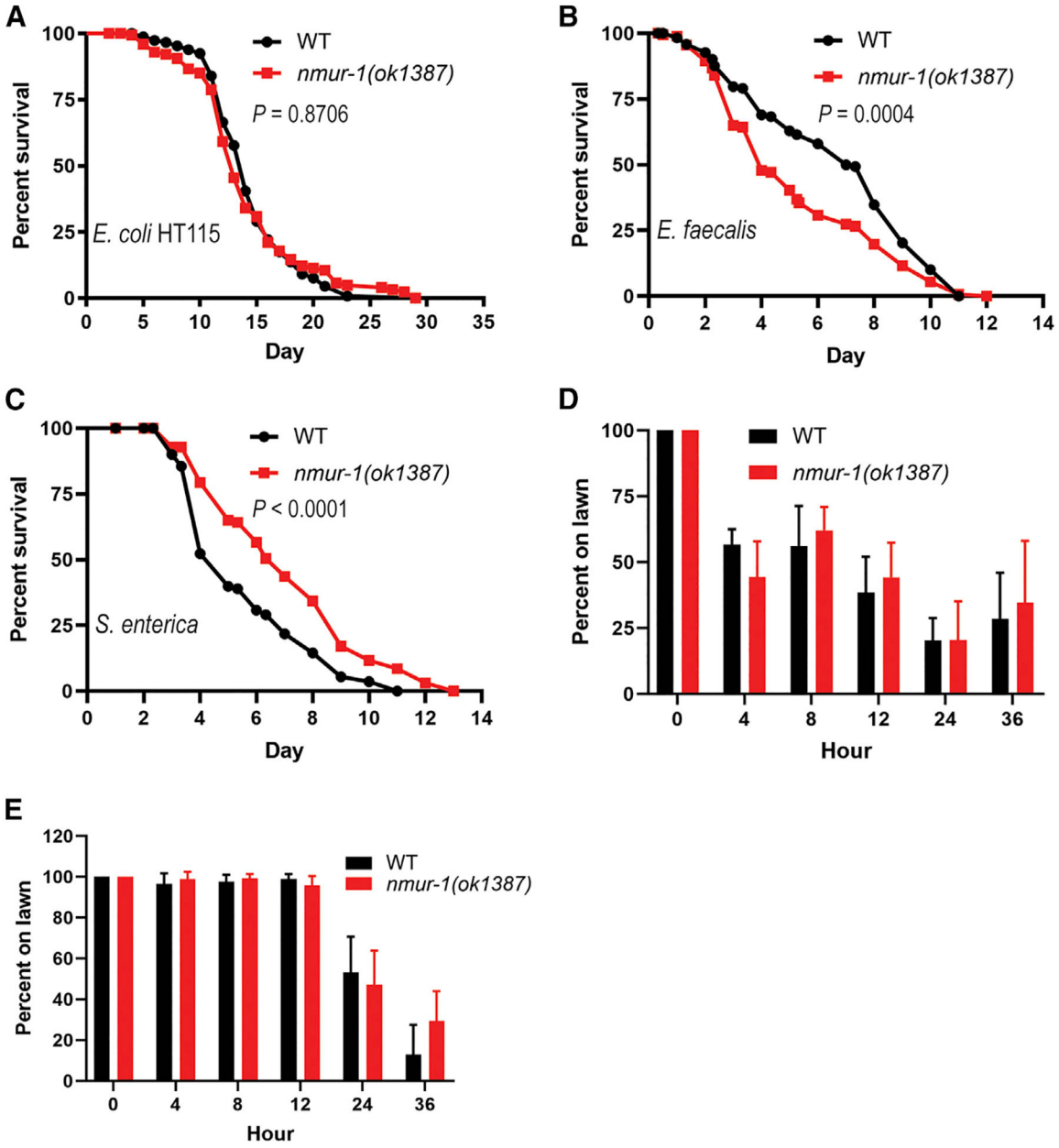

Figure 1. Functional loss of NMUR-1 differentially affects *C. elegans* survival against bacteria but does not affect pathogen avoidance behavior

(A–C) Wild-type (WT) and *nmur-1*(*ok1387*) animals were exposed to *E. coli* HT115 (A), *E. faecalis* (B), or *S. enterica* (C) and scored for survival over time. Each graph is a combination of three independent experiments. Each experiment included n = 60 animals per strain. p values represent the significance level of mutant survival relative to WT: p = 0.8706 in (A), p = 0.0004 in (B), and p < 0.0001 in (C).

(D and E) WT and *nmur-1*(*ok1387*) animals were subjected to lawn occupancy assays in which the animals were placed on a small lawn of *E. faecalis* (D) or *S. enterica* (E) in a 3.5-cm plate and monitored over time for their presence on the lawn. Each graph is a

combination of three independent experiments. Each experiment included n = 60 animals per strain. Error bars represent the standard error of the mean (SEM).

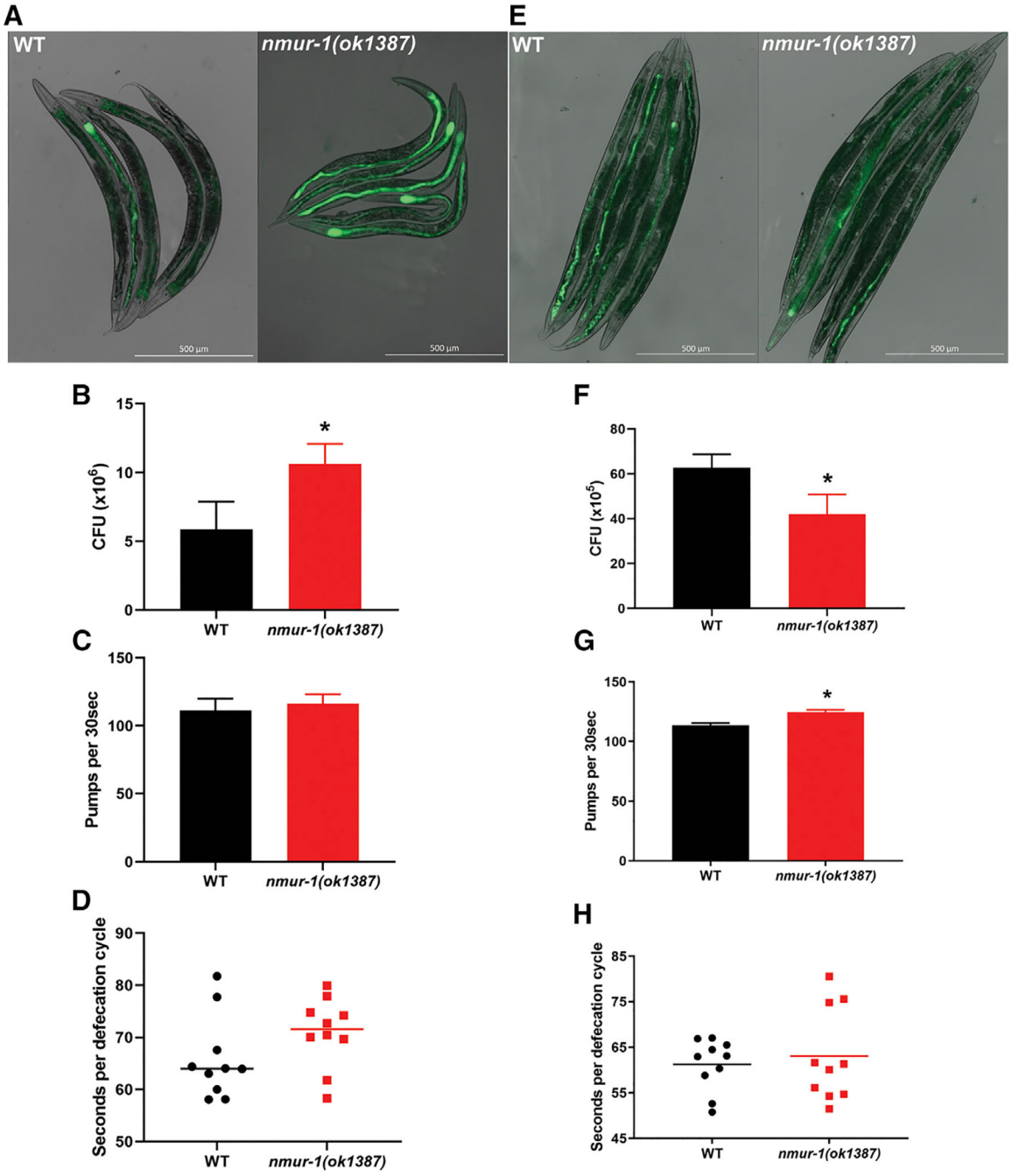

Figure 2. Functional loss of NMUR-1 changes intestinal accumulation of *E. faecalis* and *S. enterica*

(A and E) WT and *nmur-1*(*ok1387*) animals were exposed to GFP-expressing *E. faecalis* (A) or GFP-expressing *S. enterica* (E) for 24 h and then visualized using a Zeiss Axio Imager M2 fluorescence microscope. Scale bars, 500 µm.

(B and F) WT and *nmur-1*(*ok1387*) animals were exposed to *E. faecalis* (B) or *S. enterica* (F) for 24 h, and the colony-forming units (CFU) of live bacterial cells recovered from their intestines were quantified. The graph represents the combined results of three independent experiments. n = 10 animals per strain were used for each experiment. Error bars represent

SEM. p value represents the significance level of mutant gut colonization relative to WT: p = 0.0296 in (B), p = 0.0290 in (F).

(C and G) WT and *nmur-1*(*ok1387*) animals were exposed to *E. faecalis* (C) or *S. enterica* (G) for 24 h. Pharyngeal pumping rates of animals were counted as the number of pumps per 30 s. Counting was conducted in triplicate and averaged to give a pumping rate. The measurements included n = 10 adult animals per strain. Error bars represent SEM. p = 0.1068 in (C), p = 0.0006 in (G).

(D and H) WT and *nmur-1*(*ok1387*) animals were exposed to *E. faecalis* (D) or *S. enterica* (H) for 24 h. Defecation rates of animals were measured as the average time of ten intervals between two defecation cycles. The measurements included n = 10 animalsper strain.p = 0.1379in (D), p = 0.6310 in (H).

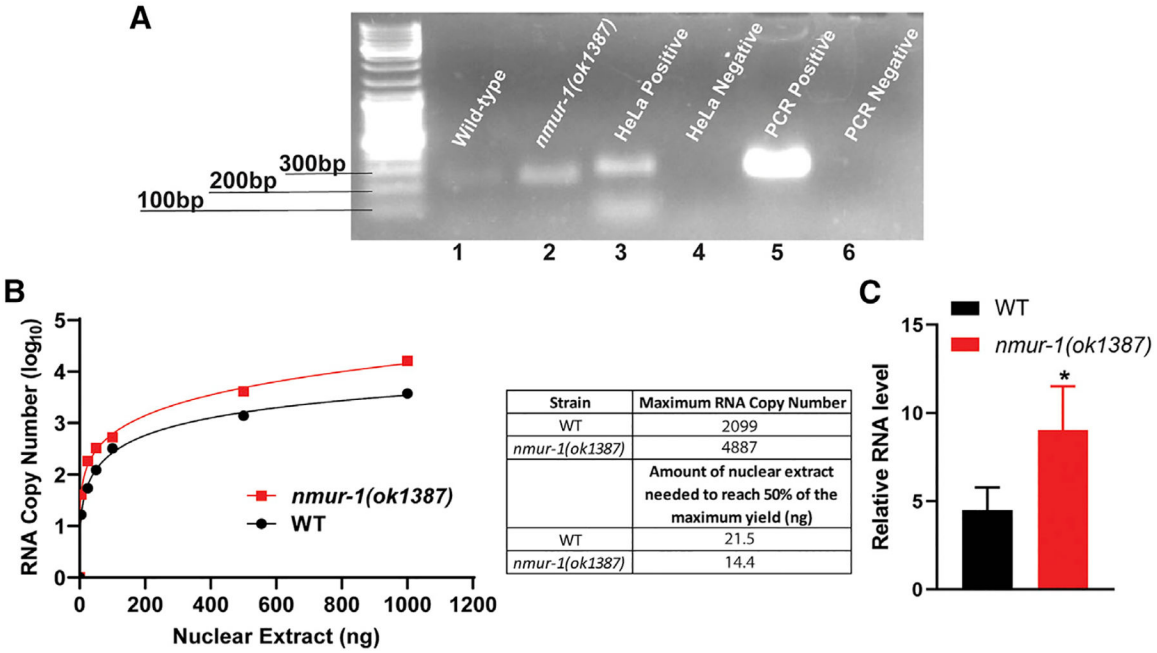

Strain	Maximum RNA Copy Number
WT	2099
nmur-1(ok1387)	4887
	Amount of nuclear extract needed to reach 50% of the maximum yield (ng)
WT	21.5
nmur-1(ok1387)	14.4

Figure 3. NMUR-1 regulates transcriptional activity

(A) *In vitro* transcription assays were performed using nuclear extract from WT or *nmur-1*(*ok1387*) animals. After transcription, RNA was purified, reverse transcribed, and amplified by PCR, followed by gel analysis. Lane 1, transcription with WT nuclear extract; lane 2, transcription with *nmur-1*(*ok1387*) nuclear extract; lane 3, transcriptional positive control (with HeLa nuclear extract); lane 4, transcriptional negative control (without any nuclear extract); lane 5, PCR positive control; lane 6, PCR negative control (without DNA template).

(B) WT and mutant nuclear extracts were titrated using the *in vitro* transcription system. The RNA copy number generated from transcription was plotted against the amount of nuclear extract used in the reaction, followed by fitting with the Michaelis-Menten model and the non-linear least-squares method to generate the titration curves and calculate titration parameters.

(C) qRT-PCR analysis of GFP expression after 2-h heat shock in *CL2070*(*dvIs70*) and *nmur-1*(*ok1387*);*CL2070*(*dvIs70*) animals. Asterisk denotes a significant difference between *CL2070*(*dvIs70*) and *nmur-1*(*ok1387*);*CL2070*(*dvIs70*) animals.

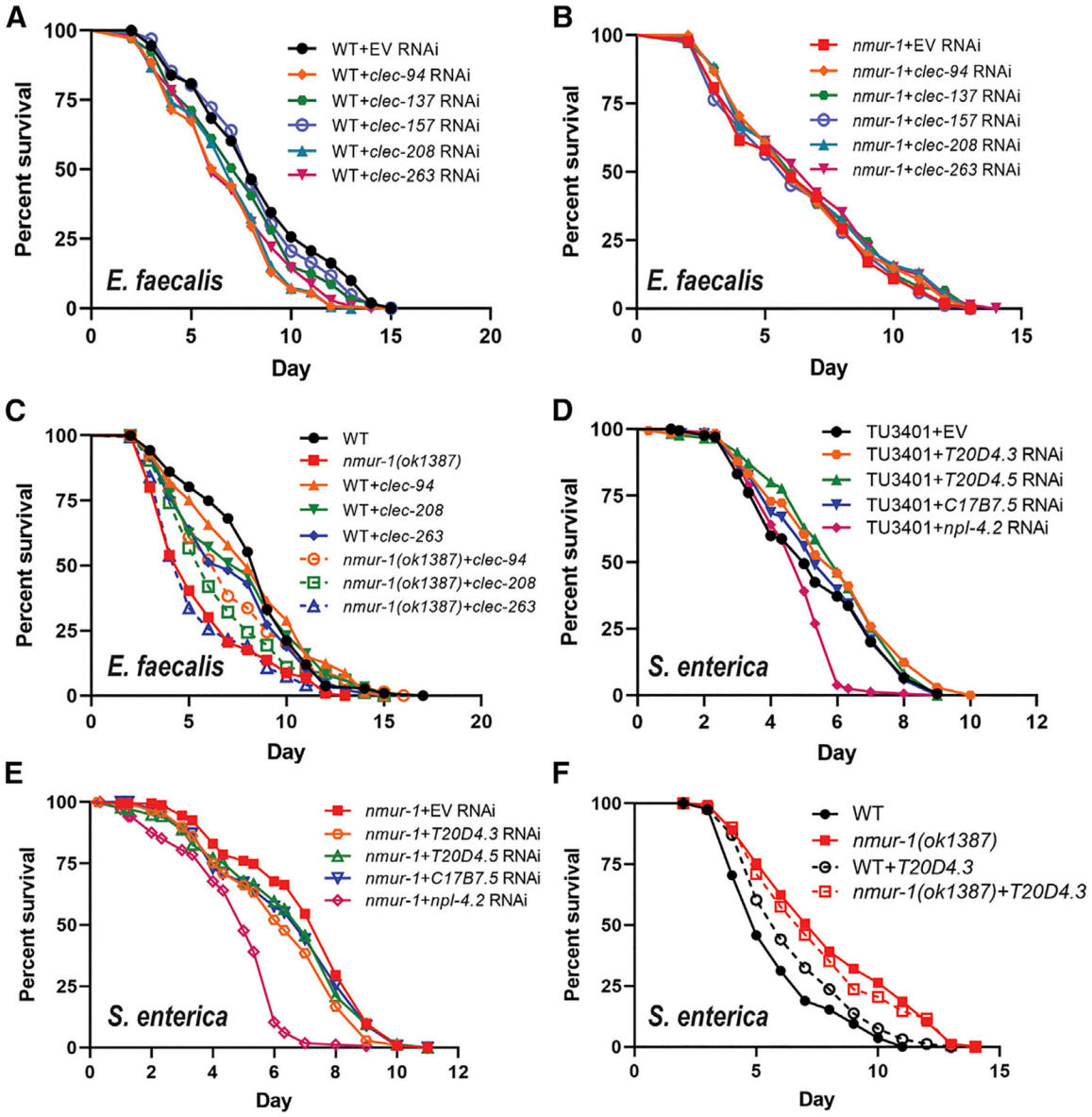

Figure 4. NMUR-1-regulated C-type lectin genes and UPR genes are required for *C. elegans* defense against *E. faecalis* and *S. enterica*, respectively

(A–B) WT (A) and *nmur-1*(*ok1387*) (B) animals grown on dsRNA for C-type lectin genes or the empty vector (EV) control were exposed to *E. faecalis* and scored for survival over time. The graphs are a combination of three independent replicates. Each experiment included n = 60 animals per strain. p values in (A) represent the significance level of RNAi treatment relative to WT + EV: WT + *clec-94*, $p < 0.0001$; WT + *clec-137*, $p = 0.0220$; WT + *clec-157*, $p = 0.3728$; WT + *clec-208*, $p < 0.0001$; WT + *clec-263*, $p < 0.0001$. p values in (B) represent the significance level of the RNAi treatment relative to *nmur-1*(*ok1387*) + EV: *nmur-1*(*ok1387*) + *clec-94*, $p = 0.3633$; *nmur-1*(*ok1387*) + *clec-137*, $p = 0.1841$; *nmur-1*(*ok1387*) + *clec-157*, $p = 0.8617$; *nmur-1*(*ok1387*) + *clec-208*, $p = 0.1348$; *nmur-1*(*ok1387*) + *clec-263*, $p = 0.1320$.

(C) WT and *nmur-1*(*ok1387*) animals in which C-type lectin expression was rescued were exposed to *E. faecalis* and scored for survival over time. All C-type lectin genes were rescued using their own promoters. The graph is a combination of three independent experiments. Each experiment included n = 60 animals per strain. p values represent the significance of the survival of rescue strains relative to *nmur-1*(*ok1378*) animals: WT, $p < 0.0001$; *nmur-1*(*ok1387*) + *clec-94*, $p < 0.0001$; *nmur-1*(*ok1387*) + *clec-208*, $p = 0.0025$; *nmur-1*(*ok1387*) + *clec-263*, $p = 0.9799$.

(D and E) TU3401(*uIs69*) (D) and *nmur-1*(*ok1387*);TU3401 (E) animals grown on dsRNA for UPR genes or the empty vector (EV) control were exposed to *S. enterica* and scored for survival over time. The graphs are a combination of three independent replicates. Each experiment included n = 60 animals per strain. p values in (D) represent the significance level of the RNAi treatment relative to the TU3401 + EV animals: TU3401 + *T20D4.3*, $p = 0.4224$; TU3401 + *T20D4.5*, $p < 0.6102$; TU3401 + *C17B7.5*, $p = 0.5905$; TU3401 + *npl-4.2*, $p < 0.0001$. p values in (E) represent the significance level of RNAi treatment relative to the *nmur-1*(*ok1387*);TU3401 + EV animals: *nmur-1*(*ok1387*);TU3401 + *T20D4.3*, $p = 0.0007$; *nmur-1*(*ok1387*);TU3401 + *T20D4.5*, $p = 0.0993$; *nmur-1*(*ok1387*);TU3401 + *C17B7.5*, $p = 0.1216$; *nmur-1*(*ok1387*);TU3401 + *npl-4.2*, $p < 0.0001$.

(F) WT, *nmur-1*(*ok1387*), and *T20D4.3* overexpression animals were exposed to *S. enterica*. *T20D4.3* was overexpressed using its own promoter. The graph is a combination of three independent experiments. Each experiment included n = 60 animals per strain. p values represent the significance of overexpression survival relative to the control animals: WT + *T20D4.3* versus WT, $p = 0.0336$; *nmur-1*(*ok1387*) + *T20D4.3* versus *nmur-1*(*ok1387*), $p = 0.5181$.

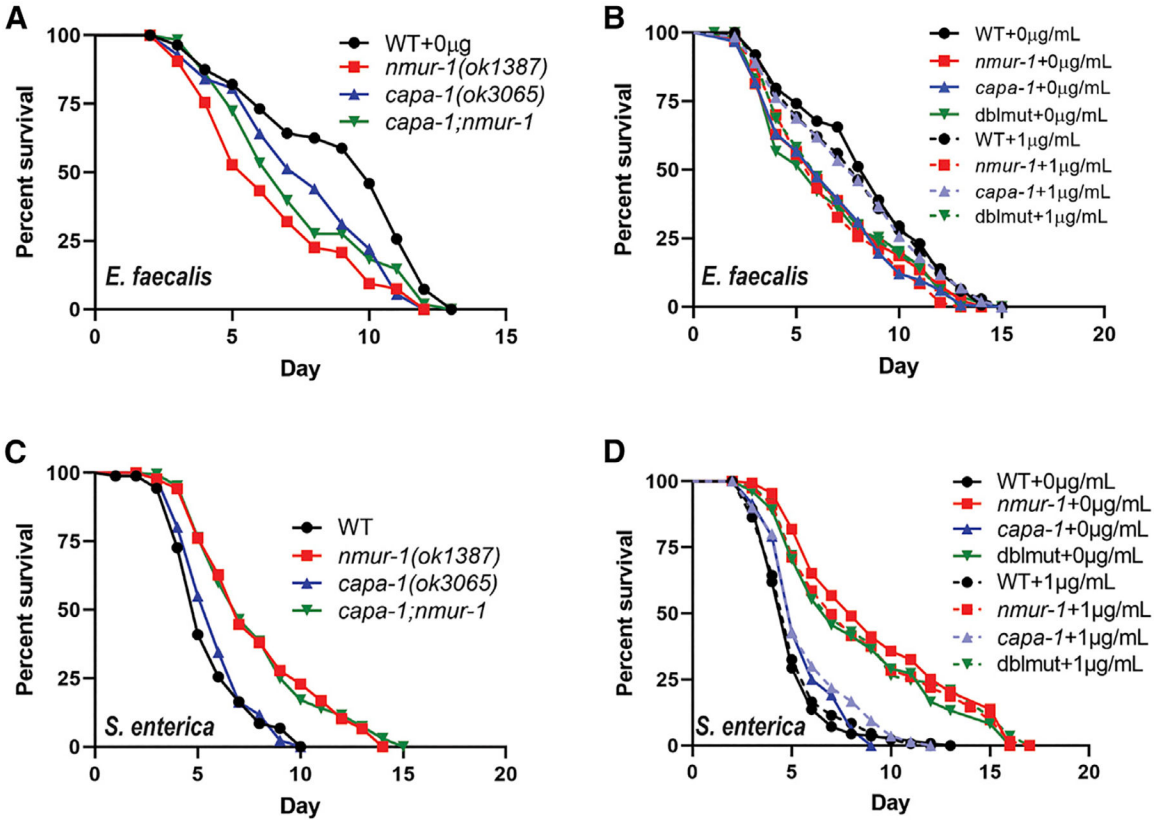

Figure 5. CAPA-1 is required for *C. elegans* defense against *E. faecalis* but not *S. enterica*

(A) WT, *nmur-1*(*ok1387*), *capa-1*(*ok3065*), and *capa-1*(*ok3065*);*nmur-1*(*ok1387*) animals were exposed to *E. faecalis* and scored for survival over time. The graph is a combination of three independent experiments. Each experiment included n = 60 animals per strain. p values represent the significance level of the mutant survival relative to the WT: *nmur-1*(*ok1387*), p = 0.0005; *capa-1*(*ok3065*), p = 0.0134; *capa-1*(*ok3065*);*nmur-1*(*ok1387*), p = 0.0028.

(B) WT, *nmur-1*(*ok1387*), *capa-1*(*ok3065*), and dblmut (*capa-1*(*ok3065*);*nmur-1*(*ok1387*)) animals were exposed to *E. faecalis* on plates containing either 0 or 1 μg of synthetic CAPA-1 peptide and scored for survival over time. The graph is a combination of three independent experiments. Each experiment included n = 60 animals per strain. p values represent the significance level of the survival for WT + 0 μg/mL versus WT + 1 μg/mL: p = 0.7467; *nmur-1*(*ok1387*) + 0 μg/mL versus *nmur-1*(*ok1387*) + 1 μg/mL: p = 0.2515; *capa-1*(*ok3065*) + 0 μg/mL versus *capa-1*(*ok3065*) + 1 μg/mL: p = 0.0005; *capa-1*(*ok3065*);*nmur-1*(*ok1387*) + 0 μg/mL versus *capa-1*(*ok3065*);*nmur-1*(*ok1387*) + 1 μg/mL: p = 0.8313.

(C) WT, *nmur-1*(*ok1387*), *capa-1*(*ok3065*), and *capa-1*(*ok3065*);*nmur-1*(*ok1387*) animals were exposed to *S. enterica* and scored for survival over time. The graph is a combination of three independent experiments. Each experiment included n = 60 animals per strain. p value represents the significance level of the mutant survival relative to WT: *nmur-1*(*ok1387*), p < 0.0001; *capa-1*(*ok3065*), p = 0.2323; *capa-1*(*ok3065*);*nmur-1*(*ok1387*), p < 0.0001.

(D) WT, *nmur-1*(*ok1387*), *capa-1*(*ok3065*), and dblmut (*capa-1*(*ok3065*);*nmur-1*(*ok1387*)) animals were exposed to *S. enterica* on plates containing either 0 or 1 μg of synthetic

CAPA-1 peptide and scored for survival over time. The graph is a combination of three independent experiments. Each experiment included n = 60 animals per strain. p values represent the significance level of the survival for WT + 0 μg/mL versus WT + 1 μg/mL: p = 0.6683; *nmur-1*(*ok1387*) + 0 μg/mL versus *nmur-1*(*ok1387*) + 1 μg/mL: p = 0.1701; *capa-1*(*ok3065*) + 0 μg/mL versus *capa-1*(*ok3065*) + 1 μg/mL: p = 0.0779; *capa-1*(*ok3065*);*nmur-1*(*ok1387*) + 0 μg/mL versus *capa-1*(*ok3065*);*nmur-1*(*ok1387*) + 1 μg/mL: p = 0.3087.

Table 1.

GO analysis of genes in *nmur-1*(*ok1387*) animals relative to wild-type animals with or without exposure to pathogens

GO term	Description	p value	FDR q value	Enrichment (N, B, n, b)
Attenuated molecular functions without exposure to pathogens				
GO:0003690	double-stranded DNA binding	2.37E–08	5.83E–05	5.59 (9,751, 169, 165, 16)
GO:0000976	transcription regulatory region sequence-specific DNA binding	3.29E–08	4.05E–05	6.41 (9,751, 129, 165, 14)
GO:0000981	DNA-binding transcription factor activity, RNA polymerase II-specific	3.66E–08	3.01E–05	7.79 (9,751, 91, 165, 12)
GO:1990837	sequence-specific double-stranded DNA binding	5.88E–08	3.62E–05	6.13 (9,751, 135, 165, 14)
GO:0001067	regulatory region nucleic acid binding	3.08E–07	1.52E–04	5.37 (9,751, 154, 165, 14)
GO:0044212	transcription regulatory region DNA binding	3.08E–07	1.26E–04	5.37 (9,751, 154, 165, 14)
GO:0003700	DNA-binding transcription factor activity	1.10E–06	3.86E–04	3.35 (9,751, 371, 165, 21)
GO:0140110	transcription regulator activity	1.97E–06	6.07E–04	3.01 (9,751, 451, 165, 23)
GO:0000977	RNA polymerase II regulatory region sequence-specific DNA binding	4.31E–06	1.18E–03	5.56 (9,751, 117, 165, 11)
GO:0001012	RNA polymerase II regulatory region DNA binding	5.51E–06	1.36E–03	5.42 (9,751, 120, 165, 11)
GO:0043565	sequence-specific DNA binding	7.12E–05	1.59E–02	2.81 (9,751, 379, 165, 18)
Attenuated molecular functions upon exposure to *E. faecalis*				
GO:0030246	carbohydrate binding	2.29E–15	5.65E–12	17.45 (10,161, 182,48, 15)
Enriched biological processes and molecular functions upon exposure to S. *enterica*				
Biological process				
GO:0006515	protein quality control for misfolded or incompletely synthesized proteins	1.35E–8	7.89E–5	137.71 (9,812, 19, 15, 4)
GO:0006516	glycoprotein catabolic process	3.45E–7	1.01E–3	196.24 (9,812, 10, 15, 3)
GO:0006517	protein deglycosylation	1.04E–6	2.03E–3	140.17 (9,812, 14, 15, 3)
GO:0009100	glycoprotein metabolic process	2E–5	2.92E–2	54.51 (9,812, 36, 15, 3)
Molecular function				
GO:0000224	peptide-N4-(N-acetyl-beta-glucosaminyl) asparagine amidase activity	2.41E–7	5.96E–4	218.04 (9,812, 9, 15,3)
GO:0016811	hydrolase activity, acting on carbon-nitrogen (but not peptide) bonds, in linear amides	2.98E–5	3.67E–2	47.86 (9,812, 41, 15, 3)

p value is computed according to the mHG model. FDR q value is the correction of the above p value for multiple testing using the Benjamini-Hochberg method. Enrichment (N, B, n, b) is defined as follows: N, total number of genes; B, total number of genes associated with a specific GO term; n, number of genes in the target set; b, number of genes in the intersection. Enrichment = (b/n)/(B/N).

Table 2.

Genes related to enriched or attenuated GO terms in *nmur-1*(*ok1387*) animals relative to wild-type animals with or without exposure to pathogens

Gene	Fold change	Adjusted p value	Gene	Fold change	Adjusted p value
Downregulated genes related to the attenuated molecular functions without exposure to pathogens					
dmd-5	3.7	3.09E–05	nhr-25	2.6	4.47E–13
unc-39	3.6	5.68E–09	ceh-43	2.5	1.35E–13
ceh-27	3.6	2.49E–11	tbx-8	2.4	1.64E–04
egl-46	3.6	9.25E–18	unc-130	2.3	1.84E–11
ces-2	3.4	1.14E–19	efl-3	2.3	2.26E–05
cnd-1	3.4	1.32E–05	sepa-1	2.1	4.00E–03
fkh-2	3.3	6.61E–07	ham-1	2.1	7.64E–13
zip-8	3.2	1.13E–06	ham-2	2.0	6.06E–08
zip-7	2.8	5.01E–11	tbx-11	2.0	6.53E–05
ref-2	2.8	1.97E–06	hbl-1	2.0	6.38E–07
eya-1	2.7	3.20E–13	ceh-32	2.0	1.20E–04
hlh-14	2.6	1.66E–07			
Downregulated genes related to the attenuated molecular functions upon exposure to *E. faecalis*					
clec-207	5.4	4.16E–15	clec-161	2.4	1.10E–04
clec-94	4.9	1.50E–12	clec-95	2.4	2.91E–04
clec-137	4.3	3.68E–10	clec-99	2.4	6.31E–05
clec-263	3.7	1.68E–08	clec-197	2.4	7.91E–04
clec-208	3.4	2.01E–07	clec-136	1.9	2.03E–02
clec-157	2.9	3.25E–06	clec-174	1.9	2.50E–03
pqn-84	2.8	2.76E–06	clec-190	1.8	1.29E–04
clec-219	2.5	2.92E–04			
Upregulated genes related to the enriched biological process protein quality control upon exposure to *S. enterica*					
C17B7.5	2.9	2.57E–14	npl-4.2	2.8	1.22E–22
T20D4.5	2.8	2.40E–15	T20D4.3	2.6	1.60E–12

Adjusted p value is the correction of the p value for multiple testing using the Benjamini-Hochberg method.

KEY RESOURCES TABLE

REAGENT or RESOURCE	SOURCE	IDENTIFIER
Bacterial and virus strains		
Escherichia coli HT115	Timmons et al. (2001)	WB Cat#WBStrain00041079
Escherichia coli OP50	Brenner (1974)	WB Cat#WBStrain00041969
Salmonella enterica SL1344	Aballay et al. (2000)	WB Cat#WBStrain00042084
S. enterica SL1344::gfp	Aballay et al. (2000)	N/A
Pseudomonas aeruginosa PA14	Tan et al. (1999)	WB Cat#WBStrain00041978
Yersinia pestis KIM5	Une and Brubaker (1984)	N/A
Enterococcus faecalis OG1RF	Dunny et al. (1978)	WB Cat#WBStrain00041967
Enterococcus faecalis OG1RF::gfp	Debroy et al. (2012)	N/A
Staphylococcus aureus MSSA476	Holden et al. (2004)	TAX Cat# 282459
Chemicals, peptides, and recombinant proteins		
oligopeptide “AFFYTPRI-NH2”	Phoenix Pharmaceuticals, Inc	N/A
Critical commercial assays		
Gentamycin Sulfate	Sigma-Aldrich	345814-M
Kanamycin monosulfate	Sigma-Aldrich	BP861
Rifampicin	Sigma-Aldrich	R3501
Triton X-100 Surfactant	Sigma-Aldrich	TX1568
Isopropyl β-D-1-thiogalactopyranoside	Sigma-Aldrich	I6758
QIAzol Lysis Reagent	Qiagen	79306
RNeasy Plus Kits	Qiagen	74134
PowerUp SYBR Green Master Mix	ThermoFisher Sci	A22918
High-Capacity cDNA Reverse Transcription Kit	ThermoFisher Sci	4368814
Deposited data		
RNA sequencing data	This Paper	GEO: GSE154324: https://www.ncbi.nlm.nih.gov/geo/query/acc.cgi?acc=GSE154324
Experimental models: organisms/strains		
C. elegans strain: Wild-type N2 (Bristol)	*Caenorhabditis elegans* Genetics Center	WB Cat#WBStrain00000001; RRID:WB-STRAIN:WBStrain00000001
C. *elegans* strain: *nmur-1*(*ok1387*)	*Caenorhabditis elegans* Genetics Center	WB Cat#WBStrain00031987; RRID:WB-STRAIN:WBStrain00031987
C. elegans strain: *capa-1* (*ok3065*)	*Caenorhabditis elegans* Genetics Center	WB Cat#WBStrain00032943; RRID:WB-STRAIN:WBStrain00032943
C. elegans strain: *CL2070*(*dvIs70*)	*Caenorhabditis elegans* Genetics Center	WB Cat#WBStrain00005096; RRID:WB-STRAIN:WBStrain00005109
C. elegans strain: TU3401[*sid-1*(*pk3321*) V; *uIs69* V]	*Caenorhabditis elegans* Genetics Center	WB Cat#WBStrain00035057; RRID:WB-STRAIN:WBStrain00024119
C. *elegans* strain: *nmur-1*(*its1672*)	Watteyne et al. (2020)	N/A
C. elegans strain: QZ0 Wild-type	Maier et al. (2010)	N/A

REAGENT or RESOURCE	SOURCE	IDENTIFIER
C. *elegans* strain: QZ58 *nmur-1*(*ok1387*)	Maier et al. (2010)	N/A
C. elegans strain: JxEx36[*nmur-1*p::gfp]	Maier et al. (2010)	N/A
C. *elegans* strain: *capa-1* (*ok3065*); *nmur-1*(*ok1387*)	This Paper	N/A
C. *elegans* strain: *nmur-1* (*ok1387*);*TU3401* [*sid-1*(*pk3321*) *V;uIs69 V]*	This Paper	N/A
C. elegans strain: CL2070(*dvIs70*); *nmur-1* (*ok1387*)	This Paper	N/A
C. elegans strain: JRS60[*clec-94p*::*clec-94*::*SL2*::*gfp*]	This Paper	N/A
C. elegans strain: JRS61[*clec-208p*::*clec-208*::*SL2*::*gfp*]	This Paper	N/A
C. elegans strain: JRS62[*clec-263p*::*clec-263*::*SL2*::*gfp*]	This Paper	N/A
C. elegans strain: JRS63[*clec-94p*::*clec-94*::*SL2*::*gfp*]; *nmur-1* (*ok1387*)	This Paper	N/A
C. elegans strain: JRS64[*clec-208p*::*clec-208*::*SL2*::*gfp*];*nmur-1* (*ok1387*)	This Paper	N/A
C. elegans strain: *JRS65*[*clec-263p*::*clec-263*::*SL2*::*gfp*];*nmur-1* (*ok1387*)	This Paper	N/A
C. elegans Strain: JRS78 [*T20D4.3p*::*T20D4.3*::*SL2*::*gfp*]	This Paper	N/A
C. elegans Strain: JRS79 [*T20D4.3p*::*T20D4.3*::*SL2*::*gfp*]; *nmur-1* (*ok1387*)	This Paper	N/A
Oligonucleotides		
See Table S6	This Paper	N/A
Recombinant DNA		
pPW02[*clec-208p*::*clec-208*::*SL2*::*gfp*]	This Paper	N/A
pPW03[*clec-263p*::*clec-263*::*SL2*::*gfp*]	This Paper	N/A
pPW04[*T20D4.3p*::*T20D4.3*::*SL2*::*gfp*]	This Paper	N/A
pPW01[*clec-94p*::*clec-94*::*SL2*::*gfp*]	This Paper	N/A
Software and algorithms		
GraphPad Prism 9	GraphPad Software	https://www.graphpad.com/
Zeiss Zen	Carl Zeiss Microscopy, LLC	https://www.zeiss.com/microscopy
ImageJ	NIH	https://imagej.nih.gov/ij/